Multibody System Dynamics
https://doi.org/10.1007/s11044-026-10175-4

RESEARCH

Parametric eigensolution sensitivity analysis using the transfer matrix method

Bo Li[1,2] · Xiao Wang[1] · Pierangelo Masarati[2]

Received: 5 January 2026 / Accepted: 8 June 2026

Abstract

The transfer matrix method has long been recognized as a computationally efficient approach for the eigenanalysis of discrete and continuous dynamic systems, particularly in structural and rotor dynamics. In this study, the transfer matrix method framework is extended to incorporate parametric sensitivity analysis, providing the foundations required for continuation-based investigations. Sensitivity analysis is performed by evaluating the parametric derivatives of eigenvalues and eigenvectors directly from the system's characteristic equation, clarifying the influence of parameter perturbations on system dynamics. To reduce computational effort, the intermediate terms required for the generic sensitivity matrix are accumulated and stored, enabling efficient evaluation of the overall sensitivity of the transfer matrix to frequency. Eigenvector normalization within the sensitivity analysis resolves the intrinsic non-uniqueness of eigenvectors and ensures consistent and stable computation of their sensitivities. The availability of consistent eigenvalue and eigenvector sensitivities naturally supports continuation procedures, enabling the systematic tracking of eigensolutions as system parameters vary and facilitating the identification of characteristic behaviors such as eigenvalue crossings and veering. Analytical sensitivity formulas inside the transfer matrix method framework and eigenvector normalization are used to address numerical challenges commonly encountered in transfer-matrix-based calculations. The methodology is verified through benchmark examples of increasing complexity, demonstrating its ability to capture critical system trends while preserving the compact structure of the transfer matrix formulation. Overall, the study demonstrates that integrating sensitivity analysis into the transfer matrix method significantly enhances its effectiveness for parametric investigations and early-stage design evaluations of complex dynamical systems, naturally supporting continuation-based analyses.

✉ P. Masarati
pierangelo.masarati@polimi.it

B. Li
bo.li@polimi.it

X. Wang
x.wang@nuaa.edu.cn

1 National Key Laboratory of Helicopter Aeromechanics, Nanjing University of Aeronautics and Astronautics, Nanjing, 210006, China

2 Department of Aerospace Science and Technology, Politecnico di Milano, Milan, 20156, Italy

Published online: 19 June 2026

Keywords Mechanical system dynamics · Eigenanalysis · Transfer matrix method · Sensitivity analysis · Eigensolution sensitivity

1 Introduction

The computation and analysis of eigensolutions, including eigenvalues and eigenvectors, are fundamental problems in multibody systems. These quantities directly determine the dynamic characteristics of systems, such as natural frequencies and mode shapes. Sensitivity analysis examines how they vary with respect to specific parameters, which is essential for the design and optimization of multibody systems [1]. The theoretical foundation of sensitivity analysis can be traced back to standard eigenvalue problems [2, 3]. A variety of methods have subsequently been developed for multibody system dynamics sensitivity analysis [4]. Sensitivity analysis methods can be categorized into numerical and analytical approaches.

Numerical methods [5–8], such as the finite difference method (FDM) and the automatic differentiation method (ADM), are generally straightforward to implement. However, FDM may suffer from numerical instability and truncation errors, depending on the step size selection. ADM is more efficient and accurate than FDM, but it requires the computation of the derivatives of the system matrices, which can be computationally expensive for large-scale systems.

Analytical eigensensitivity methods aim to derive explicit derivatives of eigenvalues and eigenvectors. Classical and recent contributions have addressed eigenvector derivatives, mode tracking, repeated eigenvalues, and analytical differentiation of eigensolutions [9–11]. Related analytical sensitivity formulations have been developed for structural and multibody-system applications [12, 13].

Among analytical approaches, the direct differentiation method (DDM) and the adjoint variable method (AVM) are commonly used in gradient-based analysis and optimization. DDM is conceptually straightforward and usually more accurate than finite differences, but it may become computationally expensive for systems with many design variables [14]. AVM improves computational efficiency by introducing adjoint variables to avoid explicit calculation of state sensitivities [15–17]; however, its application to eigenvector sensitivity analysis remains challenging.

The transfer matrix method (TMM) offers a powerful alternative for analyzing eigensolution sensitivity in mechanical systems thanks to its computational efficiency and modeling flexibility. TMM originates from the pioneering work of Holzer [18] in 1921 and was later popularized within the rotorcraft community by Myklestad [19] in 1945. Myklestad's formulation for bending-torsion analysis of rotating shafts was subsequently extended to the eigenanalysis of helicopter rotor blades. More recently, Rui et al. [20, 21] revitalized TMM and extended it to general multibody dynamics problems [22, 23]. Today, TMM is considered a powerful tool for mechanical system dynamics and is widely applied in many fields [24–26]. For one-dimensional multibody systems in particular, TMM can surpass the finite element method (FEM) in computational efficiency by propagating state vectors through the system using transfer matrices rather than assembling large coupled governing equations, significantly reducing computational complexity [20, 21].

Recent studies have further extended TMM to increasingly complex multibody dynamic systems [27]. For instance, a novel modeling and vibration analysis method [28] is developed for helicopter drivetrain systems to accurately predict dynamic behavior and coupling characteristics. Wang et al. [29] introduced a linear multibody system TMM capable of

addressing systems with ideal hinges and conservative forces, thereby broadening the applicability of TMM. Ling et al. [30] proposed an enhanced TMM-based framework for analyzing the kinetostatics and dynamics of serial-parallel compliant mechanisms with curved flexure hinges and irregular rigid bodies, demonstrating high modeling accuracy and efficiency. Dai et al. [31] combined TMM with a semi-recursive modeling approach to investigate the nonlinear force-displacement relationships of negative-stiffness devices, showing its potential for structural optimization and vibration control. Together, these developments highlight the growing relevance of TMM in tackling diverse and challenging dynamic problems.

In the TMM framework, sensitivity analysis has been investigated through recursive formulations that exploit the transfer path of multibody systems [32–34]. These approaches avoid the assembly and differentiation of large global system matrices by propagating element-level transfer matrices and their derivatives along the transfer path. They provide an important foundation for TMM-based sensitivity analysis and show the potential of recursive formulations for efficient derivative evaluation.

Despite these advances, eigensolution sensitivity within the TMM framework remains insufficiently investigated. Unlike traditional modeling strategies that lead to linear eigenvalue problems, the final eigenvalue problems derived from TMM are often highly nonlinear functions of the eigenvalues. Existing TMM-based sensitivity approaches have provided important foundations. However, compact formulations remain insufficiently developed for nonlinear TMM characteristic equations, particularly those that consistently treat both eigenvalue and eigenvector sensitivities and explicitly expose reusable transfer matrix products.

To overcome these limitations, this work proposes a sensitivity formulation for transfer-matrix eigenproblems that provides compact expressions for eigenvalue, eigenvector, and internal-state sensitivities. The formulation is based on an explicit eigenvector normalization strategy that converts the inherently singular eigenvector sensitivity problem into a slightly augmented but nonsingular system that can be solved efficiently without resorting to null-space projections or SVD-based treatments.

A further contribution is the analytical characterization of the underlying singular sensitivity structure. The explicit direct solution is primarily used to elucidate the mathematical properties of the problem and the role of the normalization condition, while the proposed augmented formulation constitutes the preferred computational strategy.

The formulation also highlights the potentially amplified sensitivity of internal states along the transfer chain and provides an efficient implementation that reuses intermediate quantities already available in standard transfer-matrix analyses.

The paper is organized as follows. Section 2 reviews the fundamental theory of TMM for eigenvalue problems and introduces the formulations of eigensolution sensitivity for TMM models. Section 3 presents the transfer matrices required for analyzing a drive system. Section 4 discusses the generalization and exploitation of eigensolution sensitivity. Section 5 provides three numerical examples, ranging from a basic disk-shaft system to branched gear systems of increasing complexity. Finally, Sect. 6 summarizes the main findings.

2 Formulation

2.1 Transfer matrix method

In the TMM, a multibody system is decomposed into simpler elements consisting of bodies and hinges, whose dynamic behavior is expressed in the form of fundamental transfer ma-

trices. The overall transfer equation of the system is obtained by successive multiplication of the transfer matrices of the individual elements, according to the system topology [35]. The characteristic equation is then derived from the overall transfer equation by applying boundary conditions to formulate the eigenvalue problem.

Let the state vector of an arbitrary element i be denoted by $\mathbf{z}_i$. The relationship between the state vectors at two ends of the system is described as

$$\mathbf{z}_O = \mathbf{U}_i \mathbf{z}_I, \tag{1}$$

where $\mathbf{z}_O$ and $\mathbf{z}_I$ are the state vectors of the output end O and input end I, respectively, and $\mathbf{U}_i(s)$ is the transfer matrix of element i, which may depend on a complex parameter $s \in \mathbb{C}$, the Laplace variable.

In a directed chain graph with n nodes ($n > 1$), labeled sequentially as $i = 1, 2, \ldots, n$, select node 1 as the input end and node n as the output end. The overall transfer matrix of the system can then be expressed as

$$\mathbf{z}_n = \Pi_{i=n}^{1} \mathbf{U}_i \mathbf{z}_1. \tag{2}$$

The general system equation can be written as

$$\begin{bmatrix} \Pi_{i=n}^{1} \mathbf{U}_i & -\mathbf{I} \end{bmatrix} \begin{Bmatrix} \mathbf{z}_1 \\ \mathbf{z}_n \end{Bmatrix} = \mathbf{0}, \tag{3}$$

or

$$\mathbf{U}_{\text{all}} \mathbf{z}_{\text{all}} = \mathbf{0}. \tag{4}$$

By imposing the boundary conditions, Eq. (4) reduces to

$$\bar{\mathbf{U}}_{\text{all}} \bar{\mathbf{z}}_{\text{all}} = \mathbf{0}, \tag{5}$$

where the reduced state vector $\bar{\mathbf{z}}_{\text{all}}$ contains only the boundary state variables not eliminated by the constraints, i.e., $\mathbf{z}_{\text{all}} = \mathbf{B}\bar{\mathbf{z}}_{\text{all}}$. Here, $\mathbf{B}$ is the transformation matrix that selects the admissible subspace of $\mathbf{z}_{\text{all}}$, and $\bar{\mathbf{U}}_{\text{all}} = \mathbf{U}_{\text{all}}\mathbf{B}$ is the corresponding reduced transfer matrix obtained by eliminating the unnecessary columns.

The eigenvalues and eigenvectors of the system are finally determined by enforcing the nonlinear eigenvalue condition

$$\det\left(\bar{\mathbf{U}}_{\text{all}}(s)\right) = 0 \tag{6}$$

and solving for the values of the Laplace variable s that satisfy it.

In the applications discussed in the rest of the manuscript, non-dissipative systems are considered. Consequently, the Laplace variable s only assumes imaginary values, i.e., $s = \mathrm{j}\omega$, with $\omega \in \mathbb{R}$. As such, the dependence of the transfer matrices on the frequency ω will usually be considered.

2.2 Eigensolution sensitivity

The sensitivity of an eigensolution to system parameters can be analyzed by considering the problem

$$\bar{\mathbf{U}}(\omega)\bar{\mathbf{z}} = \mathbf{0} \tag{7a}$$

$$\mathbf{n}^{\mathsf{H}}\bar{\mathbf{z}} = 1 \tag{7b}$$

where, for simplicity, the subscript "all" is omitted and $(\cdot)^{\mathsf{H}}$ denotes the complex conjugate transpose.

Equation (7b) represents a suitable normalization of the eigenvector. Choosing a unit Euclidean norm, i.e., $\mathbf{n} \equiv \bar{\mathbf{z}}$, is a valid (and often recommended in the literature) option when the eigenproblem of Eqs. (7a)–(7b) is solved as a nonlinear[1] problem in the unknowns $\bar{\mathbf{z}}$ and ω (as discussed, for example, in [36]). However, this choice is less convenient for sensitivity analysis. In that context, it is preferable to rescale and rotate the eigenvector such that a selected component has unit real part (unit L^{∞}-norm normalization) and zero imaginary part. A convenient choice is to select the component with the largest magnitude, here indicated as the kth element, such that $\mathrm{abs}(\bar{\mathbf{z}}(k)) \equiv \max(\mathrm{abs}(\bar{\mathbf{z}}))$. This yields a real-valued vector $\mathbf{n}$ whose elements are zero except for the kth one, which is equal to unity.

Let $(\omega_\ell, \bar{\mathbf{z}}_\ell)$ denote the ℓth eigensolution, i.e., ω_ℓ renders matrix $\bar{\mathbf{U}}$ singular, with the eigenvector $\bar{\mathbf{z}}_\ell$ lying in its nullspace. The eigenvector is then re-normalized as $\bar{\mathbf{z}}_\ell := \bar{\mathbf{z}}_\ell / \bar{\mathbf{z}}_\ell(k)$, such that, after re-normalization, $\bar{\mathbf{z}}_\ell(k) \equiv 1$. Differentiating Eqs. (7a)–(7b) with respect to a generic parameter p yields

$$\bar{\mathbf{U}}\bar{\mathbf{z}}_{\ell/p} + \bar{\mathbf{U}}_{/\omega}\omega_{\ell/p}\bar{\mathbf{z}}_\ell + \bar{\mathbf{U}}_{/p}\bar{\mathbf{z}}_\ell = \mathbf{0} \tag{8a}$$

$$\mathbf{n}^{\mathsf{T}}\bar{\mathbf{z}}_{\ell/p} = 0, \tag{8b}$$

where $\mathbf{n}^{\mathsf{T}}$ is used instead of $\mathbf{n}^{\mathsf{H}}$ since $\mathbf{n}$ is real-valued. Equations (8a)–(8b) constitute a complex-valued linear problem of order $\mathrm{size}(\bar{\mathbf{z}}) + 1$ in terms of the sensitivities $(\omega_{\ell/p}, \bar{\mathbf{z}}_{\ell/p})$. Equation (8b) is now a complex scalar constraint, which independently enforces the real and imaginary parts of $\bar{\mathbf{z}}_{\ell/p}(k)$ to vanish. The system can therefore be rearranged as

$$\begin{bmatrix} \bar{\mathbf{U}} & \bar{\mathbf{U}}_{/\omega}\bar{\mathbf{z}}_\ell \\ \mathbf{n}^{\mathsf{T}} & 0 \end{bmatrix} \begin{Bmatrix} \bar{\mathbf{z}}_{\ell/p} \\ \omega_{\ell/p} \end{Bmatrix} = \begin{Bmatrix} -\bar{\mathbf{U}}_{/p}\bar{\mathbf{z}}_\ell \\ 0 \end{Bmatrix}. \tag{9}$$

Equation (8b) thus ensures that the eigenvector varies consistently with the parameter perturbation while preserving a real, unit-valued kth component.

2.2.1 Direct solution

Since $\bar{\mathbf{z}}_\ell$ is the eigenvector of $\bar{\mathbf{U}}$ that corresponds to the eigenvalue ω_ℓ, the matrix $\bar{\mathbf{U}}$ is singular (of rank $n-1$, unless the eigenvalue has higher multiplicity, which we do not consider here; see [36] for a complete discussion of this topic). Therefore, $\bar{\mathbf{U}}\bar{\mathbf{z}}_\ell \equiv \mathbf{0}$. Consequently, Eq. (9) cannot be solved in closed form using the matrix inversion lemma (or Woodbury identity) and its variants [37].

As discussed in [36], a workaround is to introduce a non-zero scalar γ in the bottom-right corner of the matrix:

$$\begin{bmatrix} \bar{\mathbf{U}} & \bar{\mathbf{U}}_{/\omega}\bar{\mathbf{z}}_\ell \\ \mathbf{n}^{\mathsf{T}} & \gamma \end{bmatrix} \begin{Bmatrix} \bar{\mathbf{z}}_{\ell/p} \\ \omega_{\ell/p} \end{Bmatrix} = \begin{Bmatrix} -\bar{\mathbf{U}}_{/p}\bar{\mathbf{z}}_\ell \\ 0 \end{Bmatrix}, \tag{10}$$

[1] Without loss of generality, in the following examples, the nonlinearity of the eigenproblem with respect to frequency ω is polynomial, although different forms are possible; e.g., exponential, in the case of a time delay.

solve the problem, and then take the limit for $\gamma \to 0$. The resulting solution is

$$\omega_{\ell/p} = -\frac{1}{\gamma}\mathbf{n}^{\mathsf{T}}\bar{\mathbf{z}}_{\ell/p} \tag{11a}$$

$$\left(\bar{\mathbf{U}} - \frac{1}{\gamma}\bar{\mathbf{U}}_{/\omega}\bar{\mathbf{z}}_{\ell}\mathbf{n}^{\mathsf{T}}\right)\bar{\mathbf{z}}_{\ell/p} = -\bar{\mathbf{U}}_{/p}\bar{\mathbf{z}}_{\ell}, \tag{11b}$$

with $\gamma \to 0$.

Applying the generalized inversion of the sum of singular matrices described in [38] (via the SVD and spectral decomposition, along the lines of the discussion in [36]; see Appendix 6 for details), one obtains

$$\left(\bar{\mathbf{U}} - \frac{1}{\gamma}\bar{\mathbf{U}}_{/\omega}\bar{\mathbf{z}}_{\ell}\mathbf{n}^{\mathsf{T}}\right)^{-1} = \mathbf{G} + \mathbf{x}\gamma\mathbf{y}^{\mathsf{H}}, \tag{12}$$

where $\mathbf{G}$, $\mathbf{x}$, and $\mathbf{y}$ are defined in Eqs. (A.9a)–(A.9c) and (A.18a)–(A.18c) by analogy with Eq. (8) of [38]. The solution of Eqs. (11a)–(11b) is then

$$\bar{\mathbf{z}}_{\ell/p} = -\left(\mathbf{G} + \mathbf{x}\gamma\mathbf{y}^{\mathsf{H}}\right)\bar{\mathbf{U}}_{/p}\bar{\mathbf{z}}_{\ell} \overset{\lim\gamma\to 0}{=} -\mathbf{G}\bar{\mathbf{U}}_{/p}\bar{\mathbf{z}}_{\ell} \tag{13a}$$

$$\omega_{\ell/p} = \frac{1}{\gamma}\mathbf{n}^{\mathsf{T}}\left(\mathbf{G} + \mathbf{x}\gamma\mathbf{y}^{\mathsf{H}}\right)\bar{\mathbf{U}}_{/p}\bar{\mathbf{z}}_{\ell} = \left(\frac{1}{\gamma}\cancel{\mathbf{n}^{\mathsf{T}}\mathbf{G}} + \mathbf{n}^{\mathsf{T}}\mathbf{x}\mathbf{y}^{\mathsf{H}}\right)\bar{\mathbf{U}}_{/p}\bar{\mathbf{z}}_{\ell}, \tag{13b}$$

where in Eq. (13b) the term $\mathbf{n}^{\mathsf{T}}\mathbf{G} \equiv \mathbf{0}^{\mathsf{T}}$ since $\mathbf{n}$ lies in the nullspace of $\mathbf{G}^{\mathsf{H}}$ (see Corollary 1 in [38] and Eqs. (A.10d) and (A.19d)). Thus, the solution does not depend on γ, which does not enter the definition of $\mathbf{G}$, $\mathbf{x}$, or $\mathbf{y}$.

2.2.2 Computation of system matrix sensitivity

The sensitivity of the system matrix is obtained by differentiation as

$$\bar{\mathbf{U}}_{/p} = (\mathbf{UB})_{/p} = \mathbf{U}_{/p}\mathbf{B}, \tag{14}$$

since $\mathbf{B}$ is constant.

If the matrix $\mathbf{U}_k$ of only one element depends on the parameter p, then

$$\mathbf{U}_{/p} = \left[\left(\Pi_{i=n}^{k+1}\mathbf{U}_i\right)\mathbf{U}_{k/p}\left(\Pi_{i=k-1}^{1}\mathbf{U}_i\right) \qquad \mathbf{0}\right], \tag{15}$$

while dependence on frequency affects multiple matrices, resulting in

$$\mathbf{U}_{/\omega} = \left[\sum_{k=1}^{n}\left[\left(\Pi_{i=n}^{k+1}\mathbf{U}_i\right)\mathbf{U}_{k/\omega}\left(\Pi_{i=k-1}^{1}\mathbf{U}_i\right)\right] \qquad \mathbf{0}\right]. \tag{16}$$

If multiple element matrices $\mathbf{U}_i$ depend on p, Eq. (15) can be generalized in analogy with Eq. (16). We adopt the convention that $\Pi_{i=a}^{b}\mathbf{U}_i = \mathbf{I}$ if $a < b$. The zero block on the right results from the derivative of the corresponding identity matrix block, which is constant.

The product forms in Eqs. (15) and (16) explicitly expose the accumulated transfer matrix products that appear on the left and right of each local derivative. For clarity, these products

can be denoted as

$$\mathbf{L}_k^j = \Pi_{i=j}^{k+1}\mathbf{U}_i, \qquad \mathbf{R}_k = \Pi_{i=k-1}^{1}\mathbf{U}_i. \tag{17}$$

The accumulated products $\mathbf{L}_k^j$ and $\mathbf{R}_k$, with $\mathbf{L}_k \equiv \mathbf{L}_k^n$, are used in both the generic parameter sensitivity matrix $\mathbf{U}_{/p}$ and the frequency sensitivity matrix $\mathbf{U}_{/\omega}$. Therefore, they can be computed recursively, stored, and reused for different derivative evaluations, avoiding redundant reconstruction of the same intermediate transfer products.

It should be noted that $\mathbf{U}_{i/\omega}$ is non-zero only for transfer matrices that explicitly depend on ω. As will be discussed later, this dependence arises only in specific components, namely those associated with inertia or other dynamic effects.

2.2.3 Eigenvector sensitivity propagation

Once an eigensolution and its sensitivity have been computed, they can be used to propagate both the eigenvector and its sensitivity throughout the system.

The transfer relation between states k and $k+1$, expressed as

$$\mathbf{z}_{k+1} = \mathbf{U}_k\mathbf{z}_k, \tag{18}$$

implies that the state $k+1$ can be reconstructed as

$$\mathbf{z}_{k+1} = \left(\Pi_{i=k}^{1}\mathbf{U}_i\right)\mathbf{z}_1 = \mathbf{R}_{k+1}\mathbf{z}_1, \tag{19}$$

or

$$\begin{Bmatrix} \mathbf{z}_{k+1} \\ \mathbf{z}_k \\ \cdots \\ \mathbf{z}_3 \\ \mathbf{z}_2 \\ \mathbf{z}_1 \end{Bmatrix} = \begin{bmatrix} \mathbf{U}_k\mathbf{U}_{k-1}\ldots\mathbf{U}_2\mathbf{U}_1 \\ \mathbf{U}_{k-1}\ldots\mathbf{U}_2\mathbf{U}_1 \\ \cdots \\ \mathbf{U}_2\mathbf{U}_1 \\ \mathbf{U}_1 \\ \mathbf{I} \end{bmatrix}\mathbf{z}_1 = \begin{bmatrix} \mathbf{R}_{k+1} \\ \mathbf{R}_k \\ \cdots \\ \mathbf{R}_2 \\ \mathbf{R}_1 \\ \mathbf{I} \end{bmatrix}\mathbf{z}_1, \tag{20}$$

as a function of the state $\mathbf{z}_1$. The state $\mathbf{z}_1$, in turn, is reconstructed by combining the elements at node 1 of the reduced state $\bar{\mathbf{z}}$ and any associated boundary conditions at the same node. In practice, however, the state at the internal nodes can be reconstructed more efficiently in an incremental manner, directly using Eq. (18).

The sensitivity of the incremental state transfer is therefore given by

$$\mathbf{z}_{(k+1)/p} = \mathbf{U}_k\mathbf{z}_{k/p} + \left(\mathbf{U}_{k/\omega}\omega_{/p} + \mathbf{U}_{k/p}\right)\mathbf{z}_k. \tag{21}$$

The absolute sensitivity of the state transfer can be written as

$$\begin{aligned}\mathbf{z}_{(k+1)/p} &= \left(\Pi_{i=k}^{1}\mathbf{U}_i\right)\mathbf{z}_{1/p} + \sum_{j=1}^{k}\left(\Pi_{i=k}^{j+1}\mathbf{U}_i\right)\left(\omega_{/p}\mathbf{U}_{j/\omega} + \mathbf{U}_{j/p}\right)\left(\Pi_{i=j-1}^{1}\mathbf{U}_i\right)\mathbf{z}_1 \\ &= \mathbf{R}_{k+1}\mathbf{z}_{1/p} + \sum_{j=1}^{k}\mathbf{L}_j^k\left(\omega_{/p}\mathbf{U}_{j/\omega} + \mathbf{U}_{j/p}\right)\mathbf{R}_j\mathbf{z}_1,\end{aligned} \tag{22}$$

as a function of the state $\mathbf{z}_1$ and its sensitivity, $\mathbf{z}_{1/p}$. Nevertheless, as for the state reconstruction itself, the sensitivity propagation can be computed more efficiently in incremental form using Eq. (21).

3 Illustrative application: simple drive system

The proposed sensitivity analysis is demonstrated on systems composed of simple torsional elements, namely rigid disks and torsionally flexible shafts. Although essentially one-dimensional, this type of problem retains the full conceptual complexity required for illustration.

To this end, the transfer matrices of these elements and their contributions to the sensitivity analysis are first presented. A more extensive library of transfer matrices for multibody system elements can be found in [21].

3.1 Massless shaft

The transfer matrix of a massless shaft is

$$\mathbf{U}_{\mathrm{S}} = \begin{bmatrix} 1 & \dfrac{\ell}{GJ_p} \\ 0 & 1 \end{bmatrix}, \tag{23}$$

where ℓ is the shaft length and GJ_p its torsional stiffness. For convenience, GJ_p/ℓ is represented by a scalar stiffness coefficient k.

The partial derivative of the transfer matrix with respect to k is

$$\mathbf{U}_{\mathrm{S}/k} = \frac{\partial \mathbf{U}_{\mathrm{S}}}{\partial k} = \begin{bmatrix} 0 & -\dfrac{1}{k^2} \\ 0 & 0 \end{bmatrix}. \tag{24}$$

The parameter $k = GJ_p/\ell$ can be decomposed into its physical constituents, yielding

$$\frac{\partial \mathbf{U}_{\mathrm{S}}}{\partial GJ_p} = \frac{\partial \mathbf{U}_{\mathrm{S}}}{\partial k}\frac{\partial k}{\partial GJ_p} = \mathbf{U}_{\mathrm{S}/k}\frac{1}{\ell} \tag{25a}$$

$$\frac{\partial \mathbf{U}_{\mathrm{S}}}{\partial \ell} = \frac{\partial \mathbf{U}_{\mathrm{S}}}{\partial k}\frac{\partial k}{\partial \ell} = -\mathbf{U}_{\mathrm{S}/k}\frac{GJ_p}{\ell^2}, \tag{25b}$$

with $\partial k/\partial GJ_p = 1/\ell$ and $\partial k/\partial \ell = -GJ_p/\ell^2$.

While treating GJ_p as an independent parameter is legitimate (e.g., when modifying the shaft section to alter its stiffness), varying the shaft length may introduce additional geometric compatibility constraints. For example, in a drive line composed of multiple shafts connected by flexible joints and supports, altering one shaft's length typically requires corresponding adjustments in neighboring shafts to preserve the overall drive line length. In such cases, multiple transfer matrices may depend on the same parameter.

Finally, the partial derivative of the transfer matrix with respect to ω as required by Eq. (8a) is zero: $\mathbf{U}_{\mathrm{S}/\omega} = \mathbf{0}$.

3.2 Rigid disk

The transfer matrix of a rigid disk with inertia J is

$$\mathbf{U}_{\mathrm{D}} = \begin{bmatrix} 1 & 0 \\ -\omega^2 J & 1 \end{bmatrix}. \tag{26}$$

Its partial derivative with respect to J is

$$\mathbf{U}_{\mathrm{D}/J} = \frac{\partial \mathbf{U}_{\mathrm{D}}}{\partial J} = \begin{bmatrix} 0 & 0 \\ -\omega^2 & 0 \end{bmatrix}, \tag{27}$$

and with respect to ω is

$$\mathbf{U}_{\mathrm{D}/\omega} = \frac{\partial \mathbf{U}_{\mathrm{D}}}{\partial \omega} = \begin{bmatrix} 0 & 0 \\ -2\omega J & 0 \end{bmatrix}. \tag{28}$$

3.3 Combination of one rigid disk and one massless shaft

3.3.1 Eigenproblem

Consider the system

$$\mathbf{U} = \begin{bmatrix} \mathbf{U}_{\mathrm{S}}\mathbf{U}_{\mathrm{D}} & -\mathbf{I} \end{bmatrix} = \begin{bmatrix} 1-\omega^2\dfrac{J}{k} & \dfrac{1}{k} & -1 & 0 \\ -\omega^2 J & 1 & 0 & -1 \end{bmatrix}, \tag{29}$$

with clamped-free boundary conditions (free input, clamped output); the corresponding matrix $\mathbf{B}$ is

$$\mathbf{B} = \begin{bmatrix} 1 & 0 \\ 0 & 0 \\ 0 & 0 \\ 0 & 1 \end{bmatrix}, \tag{30}$$

since the only surviving variables are the tip rotation and the root reaction torque. Thus,

$$\begin{Bmatrix} \mathbf{z}_I \\ \mathbf{z}_O \end{Bmatrix} = \begin{Bmatrix} \theta_{\mathrm{tip}} \\ T_{\mathrm{tip}} \\ \theta_{\mathrm{root}} \\ T_{\mathrm{root}} \end{Bmatrix} = \begin{bmatrix} 1 & 0 \\ 0 & 0 \\ 0 & 0 \\ 0 & 1 \end{bmatrix} \begin{Bmatrix} \theta_{\mathrm{tip}} \\ T_{\mathrm{root}} \end{Bmatrix} = \mathbf{B}\bar{\mathbf{z}}. \tag{31}$$

The problem reduces to

$$\begin{bmatrix} 1-\omega^2\dfrac{J}{k} & 0 \\ -\omega^2 J & -1 \end{bmatrix} \begin{Bmatrix} \theta_{\mathrm{tip}} \\ T_{\mathrm{root}} \end{Bmatrix} = \begin{Bmatrix} 0 \\ 0 \end{Bmatrix}, \tag{32}$$

with unit-norm-eigenvector eigensolution

$$\omega = \pm\sqrt{\frac{k}{J}}, \qquad \bar{\mathbf{z}} = \begin{Bmatrix} \dfrac{1}{\sqrt{1+\omega^4 J^2}} \\ -\dfrac{\omega^2 J}{\sqrt{1+\omega^4 J^2}} \end{Bmatrix}. \tag{33}$$

The eigenvector is defined up to multiplication by a unit-norm complex factor $\mathrm{e}^{\mathrm{j}\psi}$, with arbitrary anomaly ψ.

3.3.2 Sensitivity matrix

The sensitivity problem requires computing $\bar{\mathbf{U}}_{/\omega}$ according to Eq. (16),

$$\mathbf{U}_{/\omega} = \begin{bmatrix} \cancel{\mathbf{U}_{\mathrm{S}/\omega}}\mathbf{U}_{\mathrm{D}} + \mathbf{U}_{\mathrm{S}}\mathbf{U}_{\mathrm{D}/\omega} & \mathbf{0} \end{bmatrix} = \begin{bmatrix} -2\omega\dfrac{J}{k} & 0 & 0 & 0 \\ -2\omega J & 0 & 0 & 0 \end{bmatrix}. \tag{34}$$

Multiplying by $\mathbf{B}$ gives

$$\bar{\mathbf{U}}_{/\omega} = \mathbf{U}_{/\omega}\mathbf{B} = \begin{bmatrix} -2\omega\dfrac{J}{k} & 0 \\ -2\omega J & 0 \end{bmatrix}, \tag{35}$$

so that the sensitivity problem matrix is

$$\begin{bmatrix} \bar{\mathbf{U}} & \bar{\mathbf{U}}_{/\omega}\bar{\mathbf{z}} \\ \mathbf{n}^{\mathsf{T}} & 0 \end{bmatrix} = \begin{bmatrix} 1-\omega^2\dfrac{J}{k} & 0 & -2\omega\dfrac{J}{k}\dfrac{1}{\sqrt{1+\omega^4J^2}} \\ -\omega^2 J & -1 & -2\dfrac{\omega J}{\sqrt{1+\omega^4J^2}} \\ \dfrac{(\omega^4J^2+\omega^4-1)\sqrt{1+\omega^4J^2}}{\omega^4J^2-1} & \dfrac{\omega^2\sqrt{1+\omega^4J^2}}{J(\omega^4J^2-1)} & 0 \end{bmatrix}. \tag{36}$$

Using the eigensolution of Eq. (33) yields

$$\begin{bmatrix} \bar{\mathbf{U}} & \bar{\mathbf{U}}_{/\omega}\bar{\mathbf{z}} \\ \mathbf{n}^{\mathsf{T}} & 0 \end{bmatrix} = \begin{bmatrix} 0 & 0 & \mp 2\sqrt{\dfrac{J}{k(1+k^2)}} \\ -k & -1 & \mp 2\sqrt{\dfrac{kJ}{1+k^2}} \\ \dfrac{(J^2k^2-J^2+k^2)\sqrt{1+k^2}}{J^2(k^2-1)} & \dfrac{k\sqrt{1+k^2}}{J^2(k^2-1)} & 0 \end{bmatrix}. \tag{37}$$

3.3.3 Sensitivity to shaft stiffness

For sensitivity with respect to the shaft stiffness k:

$$\mathbf{U}_{/k} = \begin{bmatrix} \mathbf{U}_{\mathrm{S}/k}\mathbf{U}_{\mathrm{D}} + \mathbf{U}_{\mathrm{S}}\cancel{\mathbf{U}_{\mathrm{D}/k}} & \mathbf{0} \end{bmatrix} = \begin{bmatrix} \omega^2\dfrac{J}{k^2} & -\dfrac{1}{k^2} & 0 & 0 \\ 0 & 0 & 0 & 0 \end{bmatrix}. \tag{38}$$

The corresponding right-hand side is

$$\begin{Bmatrix} -\bar{\mathbf{U}}_{/k}\bar{\mathbf{z}} \\ 0 \end{Bmatrix} = \begin{Bmatrix} -\omega^2\dfrac{J}{k^2}\dfrac{1}{\sqrt{1+\omega^4J^2}} \\ 0 \\ 0 \end{Bmatrix}. \tag{39}$$

Substituting the eigensolution of Eq. (33) gives

$$\left\{ \begin{array}{c} -\bar{\mathbf{U}}_{/k}\bar{\mathbf{z}} \\ 0 \end{array} \right\} = \left\{ \begin{array}{c} -\dfrac{1}{k}\dfrac{1}{\sqrt{1+k^2}} \\ 0 \\ 0 \end{array} \right\}, \tag{40}$$

and the sensitivity solution is

$$\omega_{/k} = \pm\frac{1}{2\sqrt{Jk}} \qquad \bar{\mathbf{z}}_{/k} = \left\{ \begin{array}{c} -\dfrac{k}{\left(1+k^2\right)^{3/2}} \\ -\dfrac{1}{\left(1+k^2\right)^{3/2}} \end{array} \right\}, \tag{41}$$

which coincides with the direct evaluation of the sensitivity of Eq. (33).

3.3.4 Sensitivity to disk inertia

For sensitivity with respect to the disk inertia J:

$$\mathbf{U}_{/J} = \left[\cancel{\mathbf{U}_{S/J}\mathbf{U}_D} + \mathbf{U}_S\mathbf{U}_{D/J} \qquad \mathbf{0} \right] = \begin{bmatrix} -\omega^2\dfrac{1}{k} & 0 & 0 & 0 \\ -\omega^2 & 0 & 0 & 0 \end{bmatrix}. \tag{42}$$

The corresponding right-hand side is

$$\left\{ \begin{array}{c} -\bar{\mathbf{U}}_{/J}\bar{\mathbf{z}} \\ 0 \end{array} \right\} = \left\{ \begin{array}{c} \omega^2\dfrac{1}{k}\dfrac{1}{\sqrt{1+\omega^4J^2}} \\ \omega^2\dfrac{1}{\sqrt{1+\omega^4J^2}} \\ 0 \end{array} \right\}. \tag{43}$$

Substituting the eigensolution of Eq. (33) yields

$$\left\{ \begin{array}{c} -\bar{\mathbf{U}}_{/J}\bar{\mathbf{z}} \\ 0 \end{array} \right\} = \left\{ \begin{array}{c} \dfrac{1}{J}\dfrac{1}{\sqrt{1+k^2}} \\ \dfrac{k}{J}\dfrac{1}{\sqrt{1+k^2}} \\ 0 \end{array} \right\}, \tag{44}$$

and the sensitivity solution is

$$\omega_{/J} = \mp\frac{1}{2J}\sqrt{\frac{k}{J}}, \qquad \bar{\mathbf{z}}_{/J} = \left\{ \begin{array}{c} 0 \\ 0 \end{array} \right\}, \tag{45}$$

which again coincides with the direct evaluation of the sensitivity of Eq. (33).

4 Generalization and exploitation of eigensolution sensitivity

Considering the definitions of $\mathbf{L}_k$ and $\mathbf{R}_k$ of Eq. (17), the sensitivity matrix with respect to a generic parameter p, Eq. (15), can be rewritten as

$$\mathbf{U}_{/p} = \mathbf{L}_i \mathbf{U}_{i/p} \mathbf{R}_i . \tag{46}$$

For the massless shaft of Sect. 3.1, this yields

$$\begin{aligned} \mathbf{U}_{/p} &= \begin{bmatrix} L_{i_{11}} & L_{i_{12}} \\ L_{i_{21}} & L_{i_{22}} \end{bmatrix} \begin{bmatrix} 0 & -1/k^2 \\ 0 & 0 \end{bmatrix} \begin{bmatrix} R_{i_{11}} & R_{i_{12}} \\ R_{i_{21}} & R_{i_{22}} \end{bmatrix} \\ &= \begin{bmatrix} -L_{i_{11}} R_{i_{21}}/k^2 & -L_{i_{11}} R_{i_{22}}/k^2 \\ -L_{i_{21}} R_{i_{21}}/k^2 & -L_{i_{21}} R_{i_{22}}/k^2 \end{bmatrix}, \end{aligned} \tag{47}$$

with $p := k$ of shaft i.

Similarly, for the rigid disk of Sect. 3.2, one obtains

$$\begin{aligned} \mathbf{U}_{/p} &= \begin{bmatrix} L_{i_{11}} & L_{i_{12}} \\ L_{i_{21}} & L_{i_{22}} \end{bmatrix} \begin{bmatrix} 0 & 0 \\ -\omega_\ell^2 & 0 \end{bmatrix} \begin{bmatrix} R_{i_{11}} & R_{i_{12}} \\ R_{i_{21}} & R_{i_{22}} \end{bmatrix} \\ &= \begin{bmatrix} -\omega_\ell^2 L_{i_{12}} R_{i_{11}} & -\omega_\ell^2 L_{i_{12}} R_{i_{12}} \\ -\omega_\ell^2 L_{i_{22}} R_{i_{11}} & -\omega_\ell^2 L_{i_{22}} R_{i_{12}} \end{bmatrix}, \end{aligned} \tag{48}$$

with $p := J$ of disk i.

The extension to more complex systems follows the same procedure. In all cases, the sensitivity matrix $\mathbf{U}_{/p}$ appears on the right-hand side of the linear problem in Eq. (9). As a consequence, analyzing the sensitivity of an eigensolution provides direct insight into how variations in specific parameters influence the system dynamics and can therefore guide design choices.

As an example, consider the sensitivity with respect to the stiffness of a massless shaft under free-free boundary conditions. The corresponding boundary-condition matrix is

$$\mathbf{B} = \begin{bmatrix} 1 & 0 \\ 0 & 0 \\ 0 & 1 \\ 0 & 0 \end{bmatrix}, \tag{49}$$

so that the sensitivity matrix reduces to

$$\bar{\mathbf{U}}_{/p} = \begin{bmatrix} -L_{i_{11}} R_{i_{21}}/k^2 & 0 \\ -L_{i_{21}} R_{i_{21}}/k^2 & 0 \end{bmatrix}, \tag{50}$$

and the right-hand side of Eq. (9) becomes

$$-\bar{\mathbf{U}}_{/p} \mathbf{z}_\ell = \begin{Bmatrix} L_{i_{11}} R_{i_{21}}/k^2 \bar{z}_{\ell_1} \\ L_{i_{21}} R_{i_{21}}/k^2 \bar{z}_{\ell_1} \end{Bmatrix}. \tag{51}$$

Sensitivities with respect to rigid-disk inertia or under different boundary conditions can be computed analogously.

If the objective is to minimize the effect of a change in the stiffness of a rod, the optimal choice is the rod that yields the smallest norm of the corresponding right-hand-side vector. Conversely, to maximize the effect of a stiffness variation, one should select the rod that produces the largest norm.

5 Numerical validation and examples

Three numerical examples are presented in this section to verify the proposed approach and demonstrate its applicability to complex systems. The first example is a two-degree-of-freedom disk-shaft system to demonstrate the basic concept and verify the eigensensitivity formulation. The second one is a branched drive train system with only torsional motion, which illustrates the treatment of branched transfer paths and geometric constraints. The last one is a six-branched gear system used to assess the applicability of the proposed approach to complex systems.

5.1 Finite element modeling

For verification and correlation purposes, a simple finite element model of the problems under study has been developed. Consider a set of kinematic variables $\theta_d \in \mathbb{R}^{n_d}$, representing the rotations of the n_d disks, and a set $\theta_s \in \mathbb{R}^{n_s}$, representing the rotations of the n_s shafts. Let $\mathbf{J}_d \in \mathbb{R}^{n_d \times n_d}$ be a diagonal matrix containing the inertia moments J_i of the disks, $i = 1, \ldots, n_d$, and $\mathbf{K}_s \in \mathbb{R}^{n_s \times n_s}$ a diagonal matrix containing the torsional stiffness coefficients GJ_j/ℓ_j of the shafts, $j = 1, \ldots, n_s$. Let $\mathbf{T}_d \in \mathbb{R}^{n_d \times n}$ be the matrix that maps the disk rotations to the n independent generalized coordinates $\mathbf{q} \in \mathbb{R}^n$, such that $\theta_d = \mathbf{T}_d \mathbf{q}$. In particular, if the rotation of disk j is related to that of disk i by the gear ratio $n_{i,j}$, then $\mathbf{T}_{d_{i,i}} = 1$ and $\mathbf{T}_{d_{j,i}} = n_{i,j}$. Similarly, let $\mathbf{B}_s \in \mathbb{R}^{n_s \times n}$ be the relative rotation matrix such that $\theta_s = \mathbf{B}_s \mathbf{q}$; if shaft k connects disks i and j, then $\mathbf{B}_{s_{k,i}} = -1$ and $\mathbf{B}_{s_{k,j}} = 1$.

Defining $\mathbf{J} = \mathbf{T}_d^{\mathsf{T}} \mathbf{J}_d \mathbf{T}_d$ and $\mathbf{K} = \mathbf{B}_s^{\mathsf{T}} \mathbf{K}_s \mathbf{B}_s$, the structural dynamics problem reads

$$\mathbf{J}\ddot{\mathbf{q}} + \mathbf{K}\mathbf{q} = \mathbf{0}, \tag{52}$$

and the associated generalized eigenproblem is

$$\left(-\omega^2 \mathbf{J} + \mathbf{K}\right) \mathbf{q} = \mathbf{0}. \tag{53}$$

This can be cast as a nonlinear problem by introducing the eigenvector normalization condition

$$\mathbf{n}^{\mathsf{H}} \mathbf{q} = 1, \tag{54}$$

where the normalization vector $\mathbf{n}$ is analogous to that discussed in Sect. 2.2. The corresponding sensitivity problem for the eigensolution $\{\omega_\ell, \mathbf{q}_\ell\}$, assuming unit multiplicity, is given by

$$\begin{bmatrix} -\omega_\ell^2 \mathbf{J} + \mathbf{K} & -2\omega_\ell \mathbf{J}\mathbf{q}_\ell \\ \mathbf{n}^{\mathsf{H}} & 0 \end{bmatrix} \begin{Bmatrix} \mathbf{q}_{\ell/p} \\ \omega_{\ell/p} \end{Bmatrix} = \begin{Bmatrix} -\left(-\omega_\ell^2 \mathbf{J}_{/p} + \mathbf{K}_{/p}\right) \mathbf{q}_\ell \\ 0 \end{Bmatrix}. \tag{55}$$

Fig. 1 Disk-shaft system layout

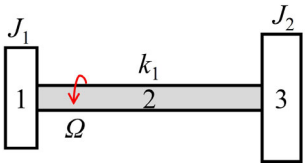

(a) Disk-shaft system

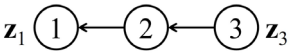

(b) Topology graph of disk-shaft system

The sensitivities of the mass and stiffness matrices are $\mathbf{J}_{/J_i} = \mathbf{T}_d^{\mathrm{T}} \mathbf{J}_{d/J_i} \mathbf{T}_d$ and $\mathbf{K}_{/k_j} = \mathbf{B}_s^{\mathrm{T}} \mathbf{K}_{s/k_j} \mathbf{B}_s$, with $k_j = GJ_j/\ell_j$, and $\mathbf{J}_{d/J_i}$ being all zeros, except for the (i, i) diagonal element equal to 1, and $\mathbf{K}_{s/k_j}$ being all zeros, except for the (j, j) diagonal element equal to 1.

5.2 Disk-shaft system

A two-degree-of-freedom disk-shaft system and its topology graph are shown in Fig. 1. The parameters of the system are given as follows: $J_1 = 1$ kg·m^2, $J_2 = 2$ kg·m^2, and $k = 1 \cdot 10^4$ N·m/rad.

The state vector of the disk-shaft system is

$$\mathbf{z}_i = \begin{Bmatrix} \theta_i \\ T_i \end{Bmatrix}. \tag{56}$$

The general equation of the disk-shaft system is

$$\begin{aligned} \mathbf{z}_1 &= \mathbf{U}_1 \mathbf{U}_2 \mathbf{U}_3 \mathbf{z}_3 \\ &= \begin{bmatrix} 1 - \omega^2 \dfrac{J_2}{k} & \dfrac{1}{k} \\ \omega^4 \dfrac{J_1 J_2}{k} - \omega^2 J_1 - \omega^2 J_2 & 1 - \omega^2 \dfrac{J_1}{k} \end{bmatrix} \mathbf{z}_3, \end{aligned} \tag{57}$$

where $\mathbf{U}_1$ and $\mathbf{U}_3$ are constructed according to Eq. (26) and $\mathbf{U}_2$ according to Eq. (23). It can be rewritten as

$$\begin{bmatrix} \mathbf{U}_1 \mathbf{U}_2 \mathbf{U}_3 & -\mathbf{I} \end{bmatrix} \begin{Bmatrix} \mathbf{z}_3 \\ \mathbf{z}_1 \end{Bmatrix} = \mathbf{0}. \tag{58}$$

Considering free-free boundary conditions, namely

$$\begin{Bmatrix} \theta_3 \\ T_3 \\ \theta_1 \\ T_1 \end{Bmatrix} = \begin{bmatrix} 1 & 0 \\ 0 & 0 \\ 0 & 1 \\ 0 & 0 \end{bmatrix} \begin{Bmatrix} \theta_3 \\ \theta_1 \end{Bmatrix}, \tag{59}$$

i.e., $T_1 = T_3 = 0$, the eigenproblem becomes

$$\bar{\mathbf{U}}\bar{\mathbf{z}} = \begin{bmatrix} 1 - \omega^2 \dfrac{J_2}{k} & -1 \\ \omega^4 \dfrac{J_1 J_2}{k} - \omega^2 J_1 - \omega^2 J_2 & 0 \end{bmatrix} \begin{Bmatrix} \theta_3 \\ \theta_1 \end{Bmatrix} = \mathbf{0}. \tag{60}$$

Solving $\det(\bar{\mathbf{U}}) = 0$ yields the non-zero solution

$$\omega = \pm \sqrt{k \left(\frac{1}{J_1} + \frac{1}{J_2} \right)}, \qquad \bar{\mathbf{z}} = \begin{Bmatrix} \dfrac{J_1}{\sqrt{J_1^2 + J_2^2}} \\ -\dfrac{J_2}{\sqrt{J_1^2 + J_2^2}} \end{Bmatrix}, \tag{61}$$

which evaluates to $\omega = 122.475$ rad/s for the given parameters.

The other eigenfrequency is zero, corresponding to a rigid-body mode,

$$\omega = 0, \qquad \bar{\mathbf{z}} = \begin{Bmatrix} \dfrac{1}{\sqrt{2}} \\ \dfrac{1}{\sqrt{2}} \end{Bmatrix}. \tag{62}$$

According to Sect. 2.2, the sensitivity of the positive eigenfrequency with respect to the design parameters is

$$\omega_{/k} = \frac{1}{2} \sqrt{\frac{1}{k} \left(\frac{1}{J_1} + \frac{1}{J_2} \right)} \tag{63a}$$

$$\omega_{/J_1} = -\frac{1}{2J_1^2} \sqrt{\frac{k}{\dfrac{1}{J_1} + \dfrac{1}{J_2}}} \tag{63b}$$

$$\omega_{/J_2} = -\frac{1}{2J_2^2} \sqrt{\frac{k}{\dfrac{1}{J_1} + \dfrac{1}{J_2}}}, \tag{63c}$$

i.e., the same results one would obtain by directly differentiating Eq. (61).

Substituting the parameter values into Eqs. (63a)–(63c) yields the sensitivity values, as shown in Table 1. Results obtained by the proposed method are compared with FDM, applying a disturbance ratio $\Delta p = 10^{-4} p$ to each parameter separately. The excellent agreement verifies the accuracy of the proposed method; minor discrepancies are attributed to the perturbation ratio in FDM. Figure 2 illustrates the evolution of the eigenfrequency and its sensitivities with respect to design parameters.

5.3 Branched drive train system

A branched drive train system and the corresponding topology graph are shown in Fig. 3. The system parameters are given in Table 2, where $n_{i,j}$ denotes the gear ratio between disks

Table 1 Disk-shaft system: eigenfrequency sensitivity with respect to design parameters (units are rad/s per the units of the respective parameters)

Method	Eigenfrequency	$k = 10^4$ N·m/rad	$J_1 = 1$ kg·m^2	$J_2 = 2$ kg·m^2
		$\omega_{/k}$, Eq. (63a)	$\omega_{/J_1}$, Eq. (63b)	$\omega_{/J_2}$, Eq. (63c)
Analytical	$\omega = 122.475$ rad/s	$6.12372 \cdot 10^{-3}$	-40.8248	-10.2062
TMM	$\omega = 122.475$ rad/s	$6.12372 \cdot 10^{-3}$	-40.8248	-10.2062
FDM	$\omega = 122.475$ rad/s	$6.12375 \cdot 10^{-3}$	-40.8250	-10.2063

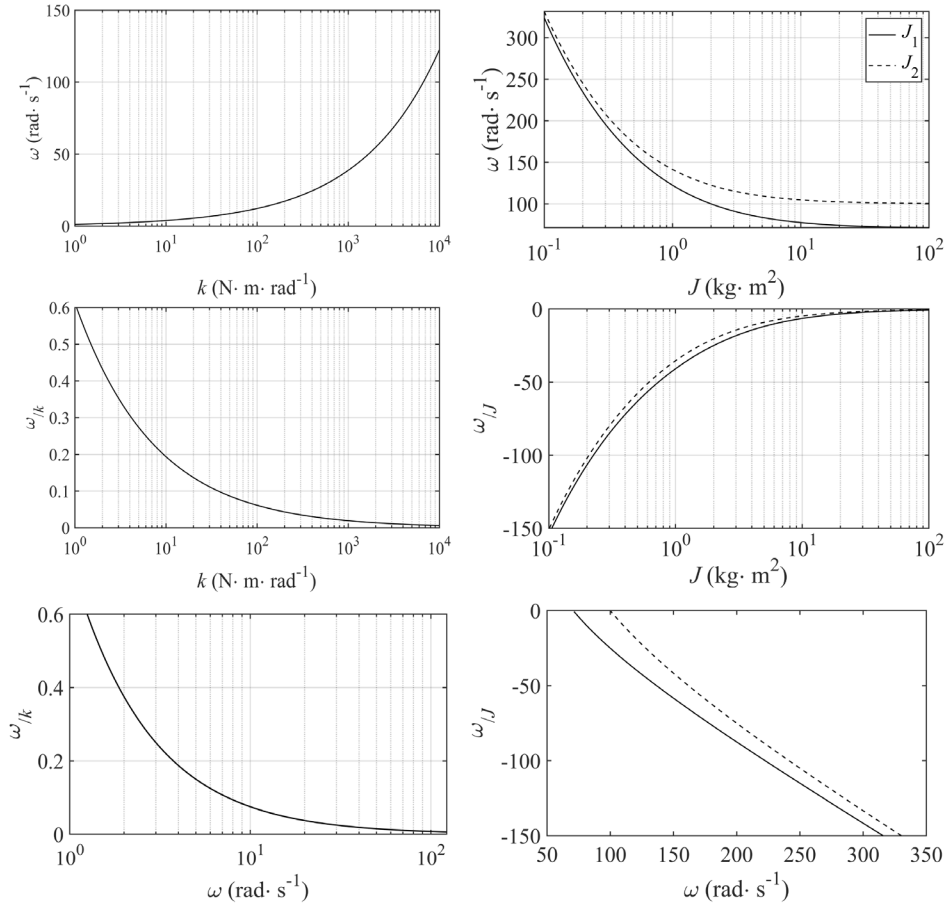

(a) Sensitivity to shaft stiffness.

(b) Sensitivity to disk inertia.

Fig. 2 Disk-shaft system: eigensolution sensitivities

i and j, such that $\omega_j = n_{i,j}\omega_i$. The general equation is

$$\mathbf{z}_1 = \mathbf{U}_1\mathbf{U}_2\mathbf{U}_3\mathbf{U}_4\mathbf{U}_5\mathbf{z}_5 + \mathbf{U}_1\mathbf{U}_2\mathbf{U}_3\mathbf{U}_6\mathbf{U}_7\mathbf{z}_7. \tag{64}$$

Fig. 3 Branched drive train system layout

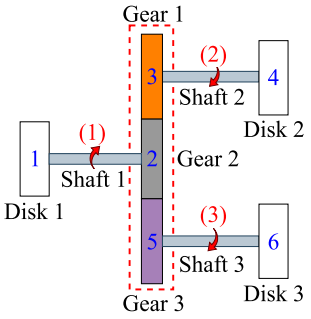

(a) Branched drive train system

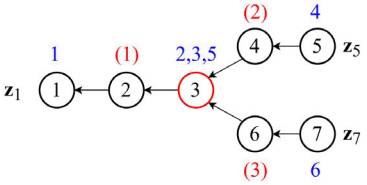

(b) Topology graph of branched drive train system

Considering the geometric constraint at the joint, Eq. (64) can be rewritten as

$$\begin{bmatrix} \mathbf{U}_1\mathbf{U}_2\mathbf{U}_3\mathbf{U}_4\mathbf{U}_5 & \mathbf{U}_1\mathbf{U}_2\mathbf{U}_3\mathbf{U}_6\mathbf{U}_7 & -\mathbf{I} \\ \mathbf{U}_{g1} & -\mathbf{U}_{g2} & \mathbf{0} \end{bmatrix} \begin{Bmatrix} \mathbf{z}_5 \\ \mathbf{z}_7 \\ \mathbf{z}_1 \end{Bmatrix} = \mathbf{0}, \tag{65}$$

where $\mathbf{U}_{g1} = \mathbf{U}_3\mathbf{U}_4\mathbf{U}_5/n_{2,3}^2$ and $\mathbf{U}_{g2} = \mathbf{U}_3\mathbf{U}_6\mathbf{U}_7/n_{2,5}^2$ are the transfer matrices used to constrain the two branches at the joint.

Considering free-free boundary conditions, namely

$$\begin{Bmatrix} \theta_5 \\ T_5 \\ \theta_7 \\ T_7 \\ \theta_1 \\ T_1 \end{Bmatrix} = \begin{bmatrix} 1 & 0 & 0 \\ 0 & 0 & 0 \\ 0 & 1 & 0 \\ 0 & 0 & 0 \\ 0 & 0 & 1 \\ 0 & 0 & 0 \end{bmatrix} \begin{Bmatrix} \theta_5 \\ \theta_7 \\ \theta_1 \end{Bmatrix}, \tag{66}$$

i.e., $T_1 = T_5 = T_7 = 0$, the eigenproblem becomes

$$\bar{\mathbf{U}}\bar{\mathbf{z}} = \mathbf{0} = \begin{bmatrix} \bar{U}_{11} & \bar{U}_{12} & -1 \\ \bar{U}_{21} & \bar{U}_{22} & 0 \\ \bar{U}_{31} & \bar{U}_{32} & 0 \end{bmatrix} \begin{Bmatrix} \mathbf{z}_5 \\ \mathbf{z}_7 \\ \mathbf{z}_1 \end{Bmatrix}, \tag{67}$$

Table 2 Branched drive train system parameters

Inertia (kg·m^2)	Stiffness (10^3 N·m/rad)	Gear ratio
$J_1, J_2, J_4, J_6 = 2$	$k_1 = 20$	$n_{2,3} = 5$
$J_3, J_5 = 1$	$k_2, k_3 = 5$	$n_{2,5} = 10$

Table 3 Branched drive train system eigensolutions

Eigenfrequency (rad/s)	Normalized disk rotation (rad)					
	θ_1	θ_2	θ_3	θ_4	θ_5	θ_6
50.000	$2.220 \cdot 10^{-16}$	$1.246 \cdot 10^{-17}$	$-6.237 \cdot 10^{-17}$	0.894	$-1.246 \cdot 10^{-16}$	−0.447
84.632	−0.267	−0.076	0.378	0.203	0.758	0.406
102.060	−0.961	0.024	−0.121	−0.023	−0.244	−0.047

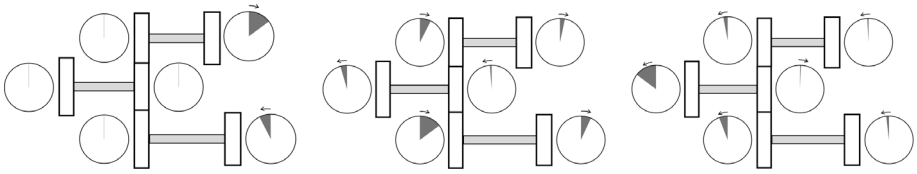

Fig. 4 Branched drive train system mode shapes

where $\bar{U}_{11} = 1 - \sigma_3 - J_4 n_{2,3}^2 \omega^2 \left(\frac{1}{k_1} - \frac{\sigma_1 + \sigma_3 - 1}{k_2 n_{2,3}^2} \right) - \sigma_1,$

$\bar{U}_{12} = 1 - \sigma_2 - J_6 n_{2,5}^2 \omega^2 \left(\frac{1}{k_1} - \frac{\sigma_1 + \sigma_2 - 1}{k_3 n_{2,5}^2} \right) - \sigma_1,$

$\bar{U}_{21} = \sigma_4 - J_1 \omega^2 - J_4 n_{2,3}^2 \omega^2 \left(\frac{\sigma_4 - J_1 \omega^2 + \sigma_6}{k_2 n_{2,3}^2} - \sigma_7 + 1 \right) + \sigma_6,$

$\bar{U}_{22} = \sigma_4 - J_1 \omega^2 - J_6 n_{2,5}^2 \omega^2 \left(\frac{\sigma_4 - J_1 \omega^2 + \sigma_5}{k_3 n_{2,5}^2} - \sigma_7 + 1 \right) + \sigma_5,$

$\bar{U}_{31} = -\frac{1}{n_{2,3}^2} \left(\frac{J_4 \omega^2}{k_2} - 1 \right), \bar{U}_{32} = -\frac{1}{n_{2,5}^2} \left(\frac{J_6 \omega^2}{k_3} - 1 \right),$

and $\sigma_1 = J_2 \omega^2 / k_1$, $\sigma_2 = J_5 n_{2,5}^2 \omega^2 / k_1$, $\sigma_3 = J_3 n_{2,3}^2 \omega^2 / k_1$, $\sigma_4 = J_2 \omega^2 (\sigma_7 - 1)$, $\sigma_5 = J_5 n_{2,5}^2 \omega^2 (\sigma_7 - 1)$, $\sigma_6 = J_3 n_{2,3}^2 \omega^2 (\sigma_7 - 1)$, $\sigma_7 = J_1 \omega^2 / k_1$.

Substituting the parameters from Table 2 yields eigenfrequencies for the first three torsional modes: 50 rad/s, 84.632 rad/s, and 102.06 rad/s. The results are identical to those obtained by FEM, demonstrating the accuracy of the TMM. The normalized eigenvectors are shown in Table 3, with the mode shapes illustrated in Fig. 4.

The first mode is dominated by torsional oscillation between θ_4 and θ_6, with a significant phase difference, while the rotations of the remaining components are comparably negligible. The second mode displays a more complex oscillatory pattern, with more participation of multiple disks. The third mode is dominated by the oscillation of disk J_1, indicating its role in this higher frequency mode.

As the FDM and TMM results are numerically identical, only the TMM results are reported in Table 4, confirming the accuracy of the proposed TMM formulation. Figure 5

Table 4 Branched drive train system: eigenfrequency sensitivity with respect to design parameters (units are rad/s per the units of the respective parameters)

Eigenfreq.		k_1	k_2	k_3	J_1	J_2	J_3	J_4	J_5	J_6
		$2{\cdot}10^4$	$5{\cdot}10^3$	$5{\cdot}10^3$	2	2	1	2	1	2
rad/s		N·m/rad	N·m/rad	N·m/rad	kg·m^2	kg·m^2	kg·m^2	kg·m^2	kg·m^2	kg·m^2
ω_1	50.000	0	$5.333{\cdot}10^{-3}$	$-3.333{\cdot}10^{-4}$	0	0	0	−13.333	0	0.833
ω_2	84.632	$1.683{\cdot}10^{-4}$	$-5.193{\cdot}10^{-4}$	$8.309{\cdot}10^{-3}$	−2.349	−0.189	1.576	0.453	−25.220	−7.251
ω_3	102.060	$2.349{\cdot}10^{-3}$	$-5.411{\cdot}10^{-5}$	$8.658{\cdot}10^{-4}$	−22.547	$-3.907{\cdot}10^{-2}$	0.326	$3.247{\cdot}10^{-2}$	−5.209	−0.519

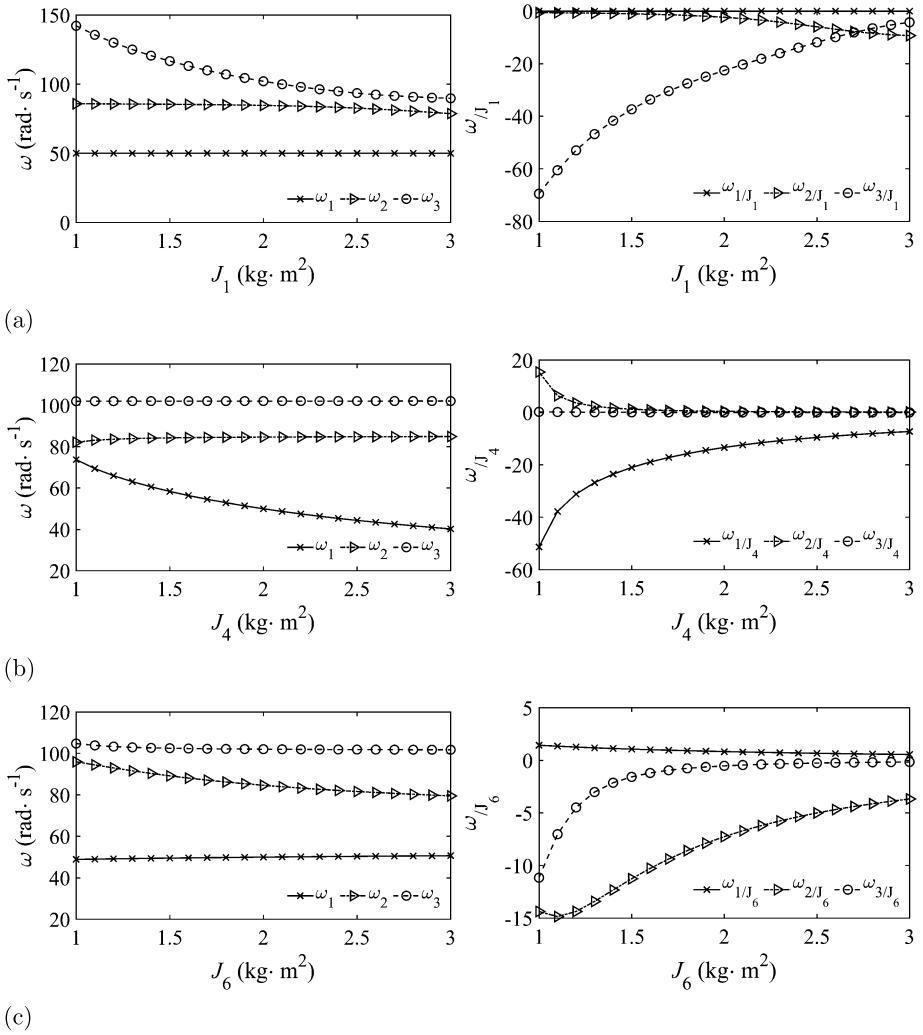

Fig. 5 Branched drive train system: eigenfrequencies and their sensitivities with respect to inertia parameters J_1, J_4, J_6

shows the frequencies and the corresponding sensitivities with respect to inertia J_1, J_4, J_6. Figure 6 exhibits the frequencies and the corresponding sensitivities with respect to stiffness k_1, k_2, k_3.

The sensitivity analysis could provide critical design insights by quantifying the influence of each parameter on the system's eigenfrequencies. The analysis demonstrates that the eigenfrequencies are not uniformly sensitive to all inertial parameters. Instead, a distinct decoupling of inertial influence is observed, where specific inertias predominantly affect specific modes. The first eigenfrequency is most sensitive to changes in inertia J_4. As shown in Fig. 5(b), the increase of J_4 leads to a marked decrease in ω_1. The second eigenfrequency is especially sensitive to J_5 compared with other inertial parameters and J_6 to a lesser ex-

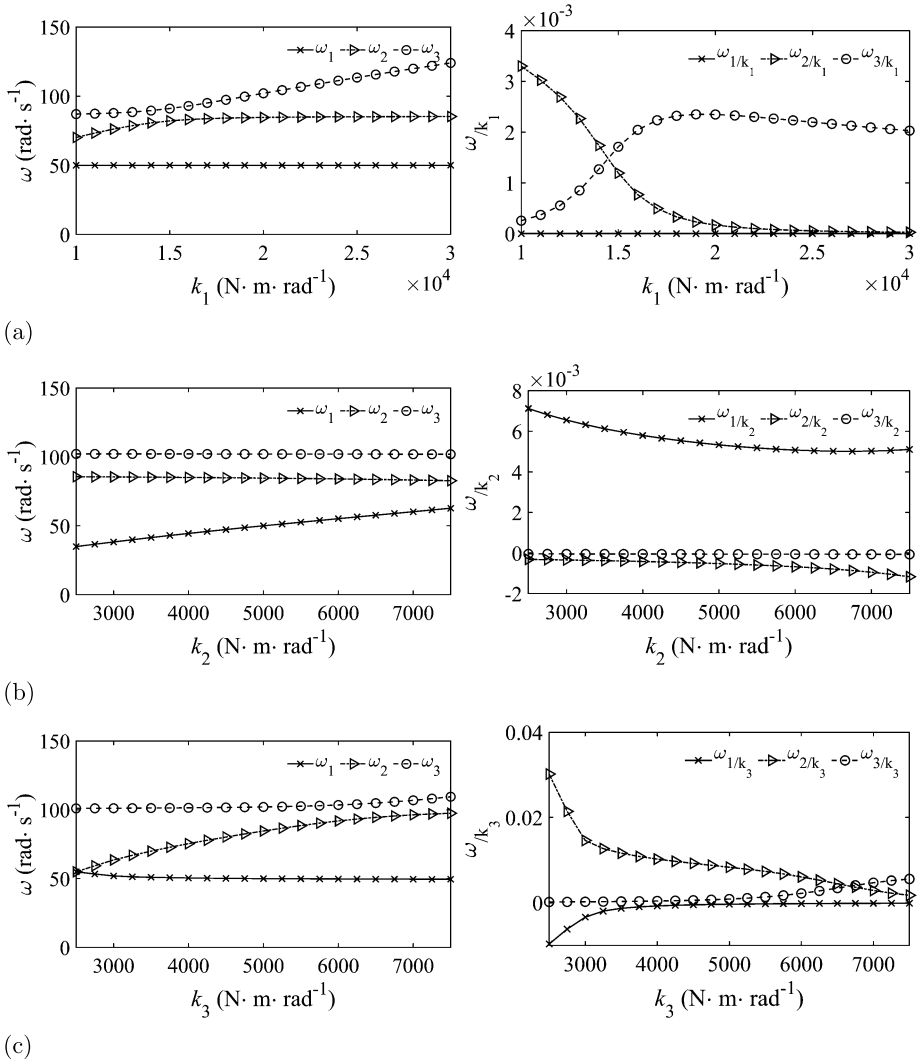

Fig. 6 Branched drive train system: eigenfrequencies and their sensitivities with respect to stiffness parameters k_1, k_2, k_3

tent. The third eigenfrequency ω_3 is predominantly governed by J_1. As is clearly shown in Fig. 5(a), ω_3 drops rapidly, as J_1 increases.

A similar phenomenon is observed for the stiffness parameters in Fig. 6. The first eigenfrequency is moderately sensitive to k_2, while slightly affected by k_3 and completely insensitive to k_1. The second eigenfrequency is mainly sensitive to k_3. It is worth noting that the stiffness k_1 influences both ω_2 and ω_3. For the early stages of design, if one wishes to shift a particular natural frequency to avoid resonance, this study identifies the most effective parameters to modify.

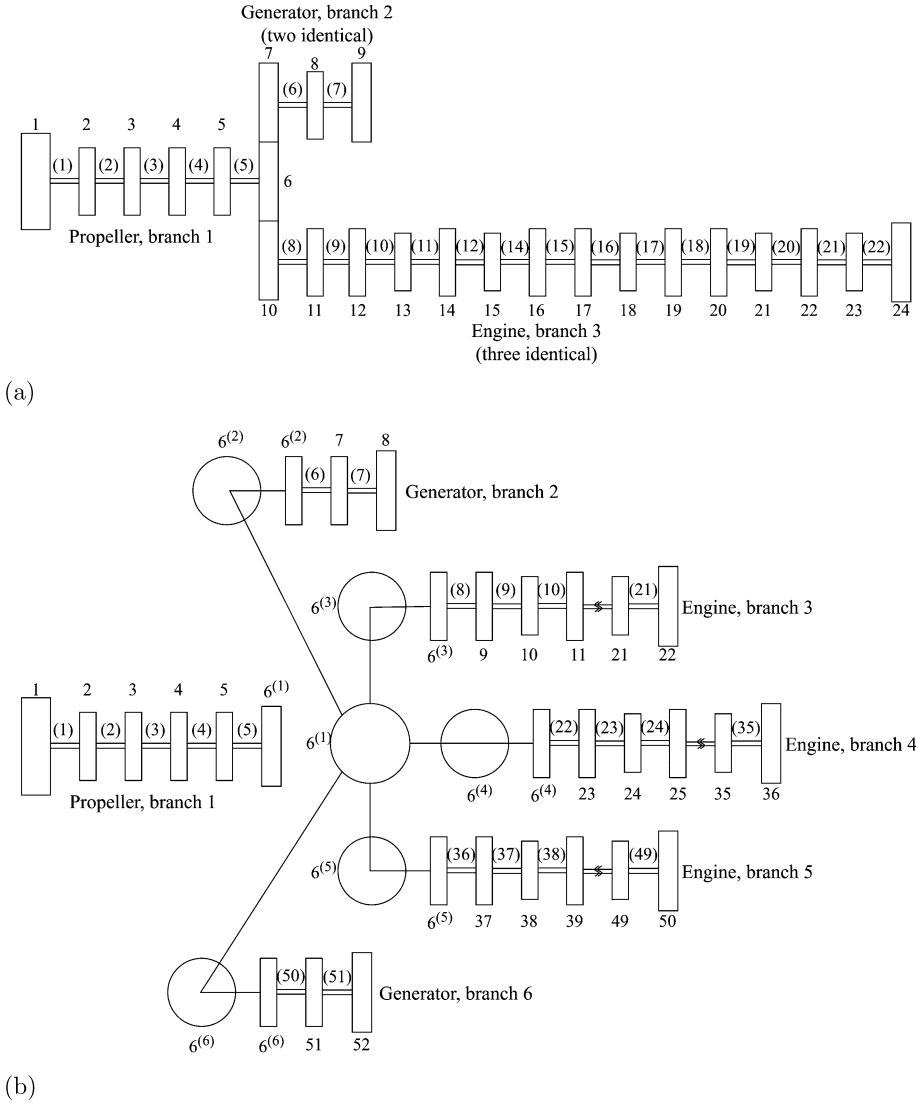

Fig. 7 Six-branch gear system layout (adapted from [39])

5.4 Six-branched gear system

A six-branched gear system adapted from [39] is considered to verify the applicability of the proposed formulation to a complex system. The model, shown in Fig. 7, contains multiple geared branches.

According to the topology of the model, node 1 is selected as the root node, while nodes 8, 22, 36, 50, and 52 are treated as the tip nodes of the five branches. The transfer relation

from the tip nodes to the root node can be expressed as

$$\begin{bmatrix}\mathbf{U}_{11} & \mathbf{U}_{12} & \mathbf{U}_{13} & \mathbf{U}_{14} & \mathbf{U}_{15} & -\mathbf{I}\end{bmatrix}\begin{Bmatrix}\mathbf{z}_8\\ \mathbf{z}_{22}\\ \mathbf{z}_{36}\\ \mathbf{z}_{50}\\ \mathbf{z}_{52}\\ \mathbf{z}_1\end{Bmatrix}=\mathbf{0}, \tag{68}$$

where $\mathbf{U}_{11}=\mathbf{U}_{D1}\mathbf{U}_{S1}\mathbf{U}_{D2}\mathbf{U}_{S2}\cdots\mathbf{U}_{D7}\mathbf{U}_{S7}\mathbf{U}_{D8}$,
$\mathbf{U}_{12}=\mathbf{U}_{D1}\mathbf{U}_{S1}\cdots\mathbf{U}_{S5}\mathbf{U}_{D6}\mathbf{U}_{D9}\mathbf{U}_{S9}\cdots\mathbf{U}_{S21}\mathbf{U}_{D22}$,
$\mathbf{U}_{13}=\mathbf{U}_{D1}\mathbf{U}_{S1}\cdots\mathbf{U}_{S5}\mathbf{U}_{D6}\mathbf{U}_{D23}\mathbf{U}_{S23}\cdots\mathbf{U}_{S35}\mathbf{U}_{D36}$,
$\mathbf{U}_{14}=\mathbf{U}_{D1}\mathbf{U}_{S1}\cdots\mathbf{U}_{S5}\mathbf{U}_{D6}\mathbf{U}_{D37}\mathbf{U}_{S37}\cdots\mathbf{U}_{S49}\mathbf{U}_{D50}$,
$\mathbf{U}_{15}=\mathbf{U}_{D1}\mathbf{U}_{S1}\cdots\mathbf{U}_{S5}\mathbf{U}_{D6}\mathbf{U}_{D51}\mathbf{U}_{S51}\mathbf{U}_{D52}$.

Considering the geometric constraint at node 6, the branch states should satisfy the compatibility relations at the geared joint. Without loss of generality, taking the branch connected to node 8 as the reference branch, the geometric constraint can be reformulated as

$$\begin{bmatrix}\mathbf{U}_{g8} & -\mathbf{U}_{g22} & \mathbf{0} & \mathbf{0} & \mathbf{0} & \mathbf{0}\\ \mathbf{U}_{g8} & \mathbf{0} & -\mathbf{U}_{g36} & \mathbf{0} & \mathbf{0} & \mathbf{0}\\ \mathbf{U}_{g8} & \mathbf{0} & \mathbf{0} & -\mathbf{U}_{g50} & \mathbf{0} & \mathbf{0}\\ \mathbf{U}_{g8} & \mathbf{0} & \mathbf{0} & \mathbf{0} & -\mathbf{U}_{g52} & \mathbf{0}\end{bmatrix}\begin{Bmatrix}\mathbf{z}_8\\ \mathbf{z}_{22}\\ \mathbf{z}_{36}\\ \mathbf{z}_{50}\\ \mathbf{z}_{52}\\ \mathbf{z}_1\end{Bmatrix}=\mathbf{0}, \tag{69}$$

where $\mathbf{U}_{g8}=\frac{\mathbf{U}_{S6}\mathbf{U}_{D7}\mathbf{U}_{S7}\mathbf{U}_{D8}}{n_{6,7}^2}$, $\mathbf{U}_{g22}=\frac{\mathbf{U}_{D9}\mathbf{U}_{S9}\cdots\mathbf{U}_{S21}\mathbf{U}_{D22}}{n_{6,9}^2}$, $\mathbf{U}_{g36}=\frac{\mathbf{U}_{D23}\mathbf{U}_{S23}\cdots\mathbf{U}_{S35}\mathbf{U}_{D36}}{n_{6,23}^2}$, $\mathbf{U}_{g50}=\frac{\mathbf{U}_{D37}\mathbf{U}_{S37}\cdots\mathbf{U}_{S49}\mathbf{U}_{D50}}{n_{6,37}^2}$, $\mathbf{U}_{g52}=\frac{\mathbf{U}_{D51}\mathbf{U}_{S51}\mathbf{U}_{D52}}{n_{6,51}^2}$.

Combining Eqs. (68) and (69) yields the expanded characteristic equation

$$\mathbf{U}(\omega,p)\begin{Bmatrix}\mathbf{z}_8\\ \mathbf{z}_{22}\\ \mathbf{z}_{36}\\ \mathbf{z}_{50}\\ \mathbf{z}_{52}\\ \mathbf{z}_1\end{Bmatrix}=\mathbf{0}. \tag{70}$$

For free-free boundary conditions, the torques at the tip and root nodes vanish, i.e., $M_8=M_{22}=M_{36}=M_{50}=M_{52}=M_1=0$. Consequently, the corresponding torque components

Table 5 Six-branch gear system natural frequencies

Mode	Present (rad/s)	FEM [39] (rad/s)	FEM [40] (rad/s)
1	26.8305	26.8301	26.8301
2	78.8965	78.8936	78.8965
3	78.8965	78.8960	78.8965
4	93.6697	93.6692	93.6667
5	103.5667	103.5667	103.5604

can be eliminated from the boundary state vector, yielding

$$\begin{Bmatrix} \theta_8 \\ M_8 \\ \theta_{22} \\ M_{22} \\ \theta_{36} \\ M_{36} \\ \theta_{50} \\ M_{50} \\ \theta_{52} \\ M_{52} \\ \theta_1 \\ M_1 \end{Bmatrix} = \begin{bmatrix} 1 & 0 & 0 & 0 & 0 & 0 \\ 0 & 0 & 0 & 0 & 0 & 0 \\ 0 & 1 & 0 & 0 & 0 & 0 \\ 0 & 0 & 0 & 0 & 0 & 0 \\ 0 & 0 & 1 & 0 & 0 & 0 \\ 0 & 0 & 0 & 0 & 0 & 0 \\ 0 & 0 & 0 & 1 & 0 & 0 \\ 0 & 0 & 0 & 0 & 0 & 0 \\ 0 & 0 & 0 & 0 & 1 & 0 \\ 0 & 0 & 0 & 0 & 0 & 0 \\ 0 & 0 & 0 & 0 & 0 & 1 \\ 0 & 0 & 0 & 0 & 0 & 0 \end{bmatrix} \begin{Bmatrix} \theta_8 \\ \theta_{22} \\ \theta_{36} \\ \theta_{50} \\ \theta_{52} \\ \theta_1 \end{Bmatrix} = \mathbf{B}\bar{\mathbf{z}}, \tag{71}$$

where $\mathbf{B}$ is the boundary matrix that retains the torsional displacement components and eliminates the corresponding torque components under the free-free boundary conditions.

The system transfer equation is converted into the reduced characteristic equation in terms of the independent boundary coordinates. Solving $\det(\bar{\mathbf{U}}) = 0$ yields the non-zero natural frequencies of the system.

The comparison of the low natural frequencies in Table 5 demonstrates the accuracy of the present formulation for the six-branch gear system. The frequencies obtained by the present method agree well with the FEM results reported in [39] and [40]. The maximum relative deviation is only 0.0061% among the listed modes, indicating that the present method is capable of accurately computing the dynamic characteristics of complex systems.

Figure 8 shows the corresponding mode shapes of the first five modes. Although the second and third modes have the same frequency within the reported numerical precision, their mode shapes are distinct.

For the parameters considered in this study, namely $p = J_i$ or $p = k_i$, the boundary conditions are independent of p. Therefore,

$$\bar{\mathbf{U}}_{/p} = \mathbf{U}_{/p}\mathbf{B}, \qquad \bar{\mathbf{U}}_{/\omega} = \mathbf{U}_{/\omega}\mathbf{B}. \tag{72}$$

Following Sect. 2.2, the relationships for the eigenvector sensitivity $\partial\bar{\mathbf{z}}_\ell/\partial p$ and the corresponding frequency derivative $\omega_{\ell/p}$ are established as follows:

$$\begin{Bmatrix} \bar{\mathbf{z}}_{\ell/J_1} \\ \omega_{\ell/J_1} \end{Bmatrix} = \begin{bmatrix} \bar{\mathbf{U}} & \bar{\mathbf{U}}_{/\omega}\bar{\mathbf{z}}_\ell \\ \mathbf{n}^{\mathrm{T}} & 0 \end{bmatrix}^{-1} \begin{Bmatrix} -\bar{\mathbf{U}}_{/J_1}\bar{\mathbf{z}}_\ell \\ 0 \end{Bmatrix}, \tag{73}$$

$$\begin{Bmatrix} \bar{\mathbf{z}}_{\ell/k_{10}} \\ \omega_{\ell/k_{10}} \end{Bmatrix} = \begin{bmatrix} \bar{\mathbf{U}} & \bar{\mathbf{U}}_{/\omega}\bar{\mathbf{z}}_\ell \\ \mathbf{n}^{\mathrm{T}} & 0 \end{bmatrix}^{-1} \begin{Bmatrix} -\bar{\mathbf{U}}_{/k_{10}}\bar{\mathbf{z}}_\ell \\ 0 \end{Bmatrix}. \tag{74}$$

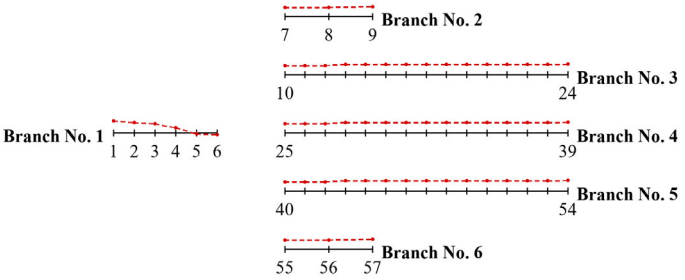

(a) Mode 1 ($\omega_1 = 26.8305$ rad/s)

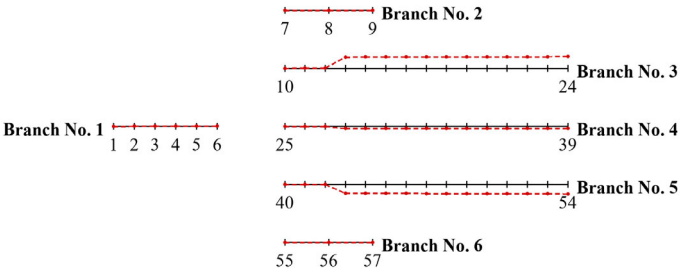

(b) Mode 2 ($\omega_2 = 78.8965$ rad/s)

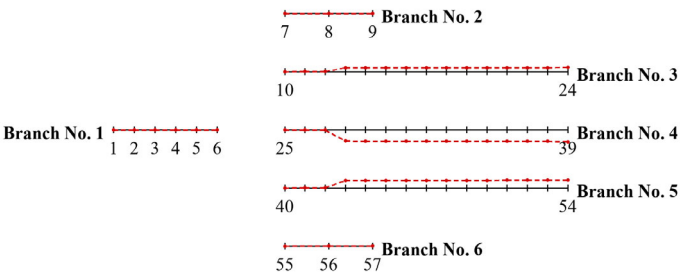

(c) Mode 3 ($\omega_3 = 78.8965$ rad/s)

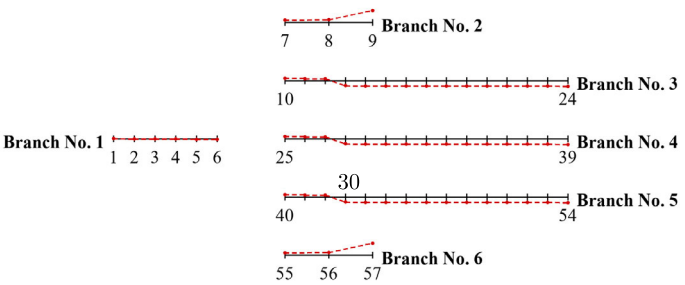

(d) Mode 4 ($\omega_4 = 93.6697$ rad/s)

Fig. 8 Six-branch gear system: mode shapes

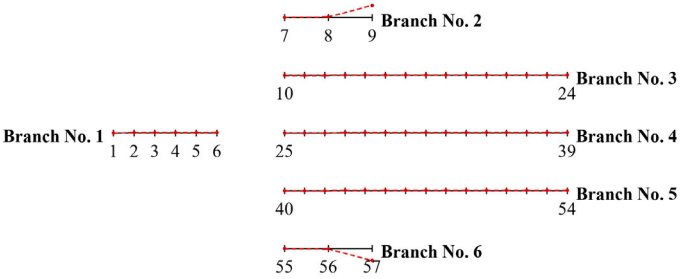

(e) Mode 5 ($\omega_5 = 103.5667$ rad/s)

Fig. 8 (*Continued*)

Table 6 Six-branch gear system: eigenfrequency sensitivity with respect to the original parameters (units are rad/s per the units of the respective parameters)

Eigenfreq.		ω_{ℓ/J_1}	$\frac{J_1}{\omega_\ell}\omega_{\ell/J_1}$	$\omega_{\ell/k_{10}}$	$\frac{k_{10}}{\omega_\ell}\omega_{\ell/k_{10}}$
ω_1	26.8305	$-2.216 \cdot 10^{-4}$	$-3.964 \cdot 10^{-1}$	$2.731 \cdot 10^{-9}$	$1.628 \cdot 10^{-3}$
ω_2	78.8965	0	0	$1.379 \cdot 10^{-6}$	$2.797 \cdot 10^{-1}$
ω_3	78.8965	0	0	$1.726 \cdot 10^{-7}$	$3.501 \cdot 10^{-2}$
ω_4	93.6697	$-1.421 \cdot 10^{-7}$	$-7.280 \cdot 10^{-5}$	$4.325 \cdot 10^{-7}$	$7.388 \cdot 10^{-2}$
ω_5	103.5667	0	0	0	0

Selected parameters: $J_1 = 4.8 \times 10^4$ lb $\cdot$ in $\cdot$ s^2 and $k_{10} = 1.6 \times 10^7$ lb $\cdot$ in/rad.

For $p = J_1$, only the derivative of the disk matrix associated with J_1 is nonzero. For $p = k_{10}$, only the derivative of the shaft matrix associated with k_{10} is nonzero. All remaining element-matrix derivatives vanish. Substituting these element-level derivatives into the sensitivity equation yields the derivatives of the eigensolutions. In this way, both the eigenvalue variation and the eigenvector variation caused by a parameter perturbation can be evaluated within the TMM framework.

The inertia J_1 and stiffness k_{10} are selected to illustrate the influence of an inertial parameter and a stiffness parameter on the eigensolutions. The eigenfrequency and eigenvector sensitivities with respect to the selected parameters are summarized in Table 6 and Table 7. The eigensolution sensitivity curves with respect to two representative parameters are shown in Fig. 9. The frequency variation is reported in terms of the ratio ω^*/ω, while the modal variation is measured by $1 - \text{MAC}$, where the superscript $(\cdot)^*$ denotes the perturbed value and MAC denotes the modal assurance criterion between the reference and perturbed eigenvectors. $1 - \text{MAC}$ remains close to zero when the mode shape is nearly unchanged.

For the inertia parameter J_1, the first mode exhibits the highest sensitivity. As J_1 increases, the first natural frequency decreases markedly, whereas the remaining modes are only slightly affected. The corresponding $1 - \text{MAC}$ curve further indicates that the eigenvector variation is primarily associated with the first mode. For the stiffness parameter k_{10}, the second natural frequency is the most sensitive. As k_{10} increases, the second natural frequency undergoes the largest variation. The fourth mode also shows a visible but weaker dependence on k_{10}, whereas the remaining modes are nearly unchanged. These results indicate that the proposed approach can accurately predict the low-frequency dynamic charac-

Table 7 Six-branch gear system: components of eigenvector sensitivity with respect to parameters J_1 and k_{10}

Eigenvector	Mode 1	Mode 2	Mode 3	Mode 4	Mode 5
$\mathbf{z}_{8/J_1}$	$2.929 \cdot 10^{-8}$	0	0	$1.188 \cdot 10^{-11}$	0
$\mathbf{z}_{22/J_1}$	$2.558 \cdot 10^{-8}$	0	0	$-1.141 \cdot 10^{-10}$	0
$\mathbf{z}_{36/J_1}$	$2.559 \cdot 10^{-8}$	0	0	$-1.140 \cdot 10^{-10}$	0
$\mathbf{z}_{50/J_1}$	$2.559 \cdot 10^{-8}$	0	0	$-1.138 \cdot 10^{-10}$	0
$\mathbf{z}_{52/J_1}$	$2.558 \cdot 10^{-8}$	0	0	$-1.141 \cdot 10^{-10}$	0
$\mathbf{z}_{1/J_1}$	$-4.441 \cdot 10^{-8}$	0	0	$-1.119 \cdot 10^{-9}$	0
$\mathbf{z}_{8/k_{10}}$	$4.726 \cdot 10^{-12}$	$3.437 \cdot 10^{-10}$	0	$-1.012 \cdot 10^{-10}$	$8.447 \cdot 10^{-16}$
$\mathbf{z}_{22/k_{10}}$	$-2.166 \cdot 10^{-11}$	$-4.009 \cdot 10^{-10}$	$1.021 \cdot 10^{-10}$	$-9.115 \cdot 10^{-10}$	$-1.371 \cdot 10^{-15}$
$\mathbf{z}_{36/k_{10}}$	$5.427 \cdot 10^{-12}$	$-3.229 \cdot 10^{-10}$	$-5.097 \cdot 10^{-11}$	$4.834 \cdot 10^{-10}$	$-1.747 \cdot 10^{-15}$
$\mathbf{z}_{50/k_{10}}$	$5.426 \cdot 10^{-12}$	$-4.981 \cdot 10^{-10}$	$-5.088 \cdot 10^{-11}$	$4.825 \cdot 10^{-10}$	0
$\mathbf{z}_{52/k_{10}}$	$5.428 \cdot 10^{-12}$	$-5.005 \cdot 10^{-10}$	$-5.103 \cdot 10^{-11}$	$4.842 \cdot 10^{-10}$	0
$\mathbf{z}_{1/k_{10}}$	$4.685 \cdot 10^{-14}$	$8.696 \cdot 10^{-12}$	0	$-2.539 \cdot 10^{-12}$	0

Selected parameters: $J_1 = 4.8 \times 10^4$ lb · in · s^2 and $k_{10} = 1.6 \times 10^7$ lb · in/rad.

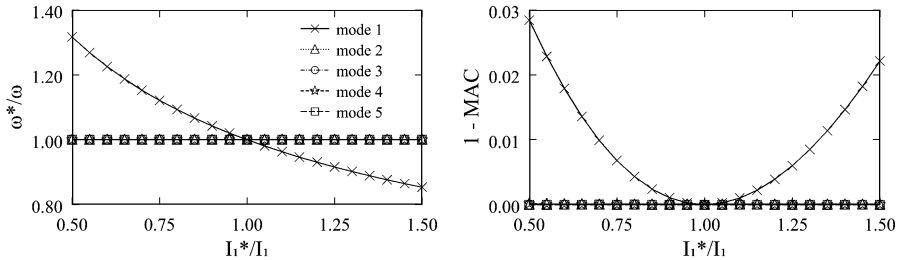

(a) sensitivity to inertia parameter J_1

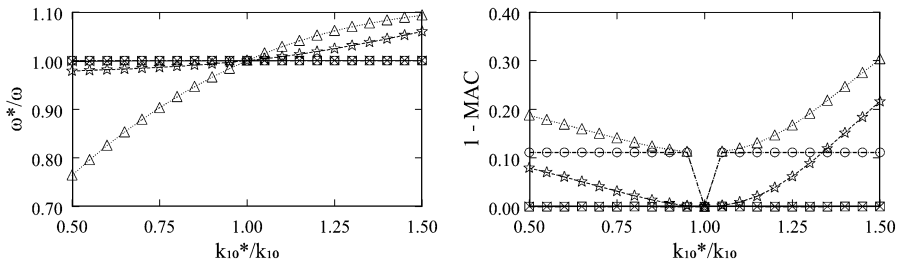

(b) sensitivity to stiffness parameter k_{10}

Fig. 9 Six-branch gear system: relative eigenvalue and eigenvector sensitivity with respect to inertia parameter J_1 and stiffness parameter k_{10}

teristics of the complex system and capture the influence of individual parameters on both eigenvalues and eigenvectors.

6 Conclusions

This work presented a sensitivity formulation for transfer-matrix eigenproblems capable of evaluating eigenvalue, eigenvector, and internal-state sensitivities within a unified framework.

A key aspect of the formulation is the explicit eigenvector normalization strategy, which removes the intrinsic indeterminacy of the eigenvector sensitivity equations and leads to a compact augmented system that can be solved efficiently using standard linear factorizations. The proposed computational procedure avoids the need for explicit null-space constructions, spectral decompositions, or singular-value-based treatments of the singular operator.

The analytical derivation of the direct solution of the singular sensitivity problem provides additional insight into the mathematical structure of the formulation. Although this direct solution is not intended as the preferred numerical implementation, it clarifies the role of the normalization condition and explains the solvability and conditioning properties of the augmented system adopted in practice.

The proposed approach is verified through several numerical examples of increasing complexity, demonstrating its applicability to complex systems. The results further show that the sensitivity of internal states may become significantly amplified along the transfer chain, even in cases where eigenvalue sensitivities remain comparatively moderate. This behavior, which is naturally captured by the proposed formulation, is relevant both from a physical interpretation standpoint and for robust numerical design and optimization procedures.

Because the sensitivity equations reuse intermediate transfer-matrix products already available during the eigensolution process, the resulting implementation remains well suited for repeated parametric analyses, continuation procedures, and gradient-based applications.

The present study is limited to non-dissipative systems. Extending the formulation to complex eigenvalues and damping parameter sensitivities will be considered in future work.

Overall, the work contributes both a practical computational framework and a clearer structural interpretation of sensitivity propagation in transfer-matrix eigenproblems.

Appendix: Inversion of linear combination of complex singular matrices

Following [38], where the inversion of the non-singular sum of singular matrices was formulated, the complex-valued problem of Eq. (11b) can be expressed as follows. Consider the problem

$$\tilde{\mathbf{A}} = \mathbf{A} + \mathbf{e}\mathbf{D}\mathbf{f}^{\mathsf{H}} \tag{A.1}$$

where, in the context of Sect. 2.2,

$$\mathbf{A} \in \mathbb{C}^{n\times n} := \bar{\mathbf{U}} \in \mathbb{C}^{n\times n} \tag{A.2a}$$

$$\mathbf{e} \in \mathbb{C}^{n\times k} := -\bar{\mathbf{U}}_{/\omega}\bar{\mathbf{z}}_{\ell} \in \mathbb{C}^{n\times 1} \tag{A.2b}$$

$$\mathbf{D} \in \mathbb{C}^{k\times k} := \frac{1}{\gamma} \in \mathbb{R} \tag{A.2c}$$

$$\mathbf{f} \in \mathbb{C}^{n\times k} := \mathbf{n} \in \mathbb{R}^{n\times 1}, \tag{A.2d}$$

with $n > r \geq 1$ and $k = n - r$ (in the present case, $r = n - 1$ and $k = 1$).

A.1 Singular value decomposition

Consider the complex SVD of matrix $\mathbf{A} \equiv \bar{\mathbf{U}}$; then

$$\mathbf{A} = \mathbf{U}\boldsymbol{\Sigma}\mathbf{V}^{\mathsf{H}} = \begin{bmatrix}\mathbf{U}_r & \mathbf{U}_k\end{bmatrix}\begin{bmatrix}\boldsymbol{\Sigma}_r & \mathbf{0}\\ \mathbf{0} & \mathbf{0}\end{bmatrix}\begin{bmatrix}\mathbf{V}_r^{\mathsf{H}}\\ \mathbf{V}_k^{\mathsf{H}}\end{bmatrix} = \mathbf{U}_r\boldsymbol{\Sigma}_r\mathbf{V}_r^{\mathsf{H}}, \tag{A.3}$$

with $\mathbf{U}_r, \mathbf{V}_r \in \mathbb{C}^{n\times r}$ and $\mathbf{U}_k, \mathbf{V}_k \in \mathbb{C}^{n\times k}$, and $\mathbf{U}^{\mathsf{H}}\mathbf{U} = \mathbf{I}$, $\mathbf{V}^{\mathsf{H}}\mathbf{V} = \mathbf{I}$, which implies $\mathbf{U}_r^{\mathsf{H}}\mathbf{U}_r = \mathbf{I}$, $\mathbf{U}_k^{\mathsf{H}}\mathbf{U}_k = \mathbf{I}$, and $\mathbf{U}_r^{\mathsf{H}}\mathbf{U}_k = \mathbf{0}$, and $\mathbf{V}_r^{\mathsf{H}}\mathbf{V}_r = \mathbf{I}$, $\mathbf{V}_k^{\mathsf{H}}\mathbf{V}_k = \mathbf{I}$, and $\mathbf{V}_r^{\mathsf{H}}\mathbf{V}_k = \mathbf{0}$, and finally $\boldsymbol{\Sigma}_r \in \mathbb{R}^{r\times r}$ diagonal, with strictly greater than zero diagonal elements. We can rewrite matrix $\tilde{\mathbf{A}}$ as

$$\tilde{\mathbf{A}} = \mathbf{A} + \mathbf{e}\mathbf{D}\mathbf{f}^{\mathsf{H}} = \mathbf{U}_r\boldsymbol{\Sigma}_r\mathbf{V}_r^{\mathsf{H}} + \mathbf{e}\mathbf{D}\mathbf{f}^{\mathsf{H}} = \begin{bmatrix}\mathbf{U}_r & \mathbf{e}\end{bmatrix}\begin{bmatrix}\boldsymbol{\Sigma}_r & \mathbf{0}\\ \mathbf{0} & \mathbf{D}\end{bmatrix}\begin{bmatrix}\mathbf{V}_r^{\mathsf{H}}\\ \mathbf{f}^{\mathsf{H}}\end{bmatrix}. \tag{A.4}$$

Under the assumption that the columns of $\mathbf{A}$ and $\mathbf{e}$ span $\mathbb{C}^n$, matrix $[\mathbf{U}_r, \mathbf{e}]$ is invertible; in fact,

$$\begin{bmatrix}\mathbf{U}_r^{\mathsf{H}}\\ \mathbf{U}_k^{\mathsf{H}}\end{bmatrix}\begin{bmatrix}\mathbf{U}_r & \mathbf{e}\end{bmatrix} = \begin{bmatrix}\mathbf{U}_r^{\mathsf{H}}\mathbf{U}_r & \mathbf{U}_r^{\mathsf{H}}\mathbf{e}\\ \mathbf{U}_k^{\mathsf{H}}\mathbf{U}_r & \mathbf{U}_k^{\mathsf{H}}\mathbf{e}\end{bmatrix} = \begin{bmatrix}\mathbf{I} & \mathbf{U}_r^{\mathsf{H}}\mathbf{e}\\ \mathbf{0} & \mathbf{U}_k^{\mathsf{H}}\mathbf{e}\end{bmatrix}, \tag{A.5}$$

i.e.,

$$\begin{bmatrix}\mathbf{U}_r & \mathbf{e}\end{bmatrix}^{-1} = \begin{bmatrix}\mathbf{I} & \mathbf{U}_r^{\mathsf{H}}\mathbf{e}\\ \mathbf{0} & \mathbf{U}_k^{\mathsf{H}}\mathbf{e}\end{bmatrix}^{-1}\begin{bmatrix}\mathbf{U}_r^{\mathsf{H}}\\ \mathbf{U}_k^{\mathsf{H}}\end{bmatrix} = \begin{bmatrix}\mathbf{U}_r^{\mathsf{H}} - \mathbf{U}_r^{\mathsf{H}}\mathbf{e}\left(\mathbf{U}_k^{\mathsf{H}}\mathbf{e}\right)^{-1}\mathbf{U}_k^{\mathsf{H}}\\ \left(\mathbf{U}_k^{\mathsf{H}}\mathbf{e}\right)^{-1}\mathbf{U}_k^{\mathsf{H}}\end{bmatrix}. \tag{A.6}$$

Similarly, under the assumption that the columns of $\mathbf{A}^{\mathsf{H}}$ and $\mathbf{f}$ span $\mathbb{C}^n$, matrix $[\mathbf{V}_r, \mathbf{f}]^{\mathsf{H}}$ is invertible; in fact,

$$\begin{bmatrix}\mathbf{V}_r & \mathbf{f}\end{bmatrix}^{-\mathsf{H}} = \begin{bmatrix}\mathbf{V}_r^{\mathsf{H}}\\ \mathbf{f}^{\mathsf{H}}\end{bmatrix}^{-1} = \begin{bmatrix}\mathbf{V}_r - \mathbf{V}_k\left(\mathbf{f}^{\mathsf{H}}\mathbf{V}_k\right)^{-1}\mathbf{f}^{\mathsf{H}}\mathbf{V}_r & \mathbf{V}_k\left(\mathbf{f}^{\mathsf{H}}\mathbf{V}_k\right)^{-1}\end{bmatrix}. \tag{A.7}$$

The inverse of matrix $\tilde{\mathbf{A}}$ is thus

$$\begin{aligned}
\tilde{\mathbf{A}}^{-1} &= \begin{bmatrix}\mathbf{V}_r^{\mathsf{H}}\\ \mathbf{f}^{\mathsf{H}}\end{bmatrix}^{-1}\begin{bmatrix}\boldsymbol{\Sigma}_r & \mathbf{0}\\ \mathbf{0} & \mathbf{D}\end{bmatrix}^{-1}\begin{bmatrix}\mathbf{U}_r & \mathbf{e}\end{bmatrix}^{-1}\\
&= \begin{bmatrix}\mathbf{V}_r - \mathbf{V}_k\left(\mathbf{f}^{\mathsf{H}}\mathbf{V}_k\right)^{-1}\mathbf{f}^{\mathsf{H}}\mathbf{V}_r & \mathbf{V}_k\left(\mathbf{f}^{\mathsf{H}}\mathbf{V}_k\right)^{-1}\end{bmatrix}\begin{bmatrix}\boldsymbol{\Sigma}_r^{-1} & \mathbf{0}\\ \mathbf{0} & \mathbf{D}^{-1}\end{bmatrix}\\
&\quad\times\begin{bmatrix}\mathbf{U}_r^{\mathsf{H}} - \mathbf{U}_r^{\mathsf{H}}\mathbf{e}\left(\mathbf{U}_k^{\mathsf{H}}\mathbf{e}\right)^{-1}\mathbf{U}_k^{\mathsf{H}}\\ \left(\mathbf{U}_k^{\mathsf{H}}\mathbf{e}\right)^{-1}\mathbf{U}_k^{\mathsf{H}}\end{bmatrix}\\
&= \left(\mathbf{V}_r - \mathbf{V}_k\left(\mathbf{f}^{\mathsf{H}}\mathbf{V}_k\right)^{-1}\mathbf{f}^{\mathsf{H}}\mathbf{V}_r\right)\boldsymbol{\Sigma}_r^{-1}\left(\mathbf{U}_r^{\mathsf{H}} - \mathbf{U}_r^{\mathsf{H}}\mathbf{e}\left(\mathbf{U}_k^{\mathsf{H}}\mathbf{e}\right)^{-1}\mathbf{U}_k^{\mathsf{H}}\right)\\
&\quad+\mathbf{V}_k\left(\mathbf{f}^{\mathsf{H}}\mathbf{V}_k\right)^{-1}\mathbf{D}^{-1}\left(\mathbf{U}_k^{\mathsf{H}}\mathbf{e}\right)^{-1}\mathbf{U}_k^{\mathsf{H}}\\
&= \mathbf{G} + \mathbf{x}\mathbf{D}^{-1}\mathbf{y}^{\mathsf{H}},
\end{aligned} \tag{A.8}$$

with

$$\mathbf{G} = \left(\mathbf{V}_r - \mathbf{V}_k \left(\mathbf{f}^{\mathsf{H}}\mathbf{V}_k\right)^{-1} \mathbf{f}^{\mathsf{H}}\mathbf{V}_r\right) \boldsymbol{\Sigma}_r^{-1} \left(\mathbf{U}_r^{\mathsf{H}} - \mathbf{U}_r^{\mathsf{H}}\mathbf{e} \left(\mathbf{U}_k^{\mathsf{H}}\mathbf{e}\right)^{-1} \mathbf{U}_k^{\mathsf{H}}\right) \tag{A.9a}$$

$$\mathbf{x} = \mathbf{V}_k \left(\mathbf{f}^{\mathsf{H}}\mathbf{V}_k\right)^{-1} \tag{A.9b}$$

$$\mathbf{y} = \mathbf{U}_k \left(\mathbf{e}^{\mathsf{H}}\mathbf{U}_k\right)^{-1}. \tag{A.9c}$$

It is worth noticing that, along the lines of Corollary 1 in [38],

$$\mathbf{A}\mathbf{x} = \mathbf{U}_r \boldsymbol{\Sigma}_r \cancel{\mathbf{V}_r^{\mathsf{H}}\mathbf{V}_k} \left(\mathbf{f}^{\mathsf{H}}\mathbf{V}_k\right)^{-1} = \mathbf{0} \tag{A.10a}$$

$$\mathbf{y}^{\mathsf{H}}\mathbf{A} = \left(\mathbf{U}_k^{\mathsf{H}}\mathbf{e}\right)^{-1} \cancel{\mathbf{U}_k^{\mathsf{H}}\mathbf{U}_r} \boldsymbol{\Sigma}_r \mathbf{V}_r^{\mathsf{H}} = \mathbf{0} \tag{A.10b}$$

$$\begin{aligned}
\mathbf{G}\mathbf{e} &= \left(\mathbf{V}_r - \mathbf{V}_k \left(\mathbf{f}^{\mathsf{H}}\mathbf{V}_k\right)^{-1} \mathbf{f}^{\mathsf{H}}\mathbf{V}_r\right) \boldsymbol{\Sigma}_r^{-1} \left(\mathbf{U}_r^{\mathsf{H}} - \mathbf{U}_r^{\mathsf{H}}\mathbf{e} \left(\mathbf{U}_k^{\mathsf{H}}\mathbf{e}\right)^{-1} \mathbf{U}_k^{\mathsf{H}}\right) \mathbf{e} \\
&= \left(\mathbf{V}_r - \mathbf{V}_k \left(\mathbf{f}^{\mathsf{H}}\mathbf{V}_k\right)^{-1} \mathbf{f}^{\mathsf{H}}\mathbf{V}_r\right) \boldsymbol{\Sigma}_r^{-1} \left(\mathbf{U}_r^{\mathsf{H}}\mathbf{e} - \mathbf{U}_r^{\mathsf{H}}\mathbf{e} \left(\mathbf{U}_k^{\mathsf{H}}\mathbf{e}\right)^{-1} \mathbf{U}_k^{\mathsf{H}}\mathbf{e}\right) \\
&= \left(\mathbf{V}_r - \mathbf{V}_k \left(\mathbf{f}^{\mathsf{H}}\mathbf{V}_k\right)^{-1} \mathbf{f}^{\mathsf{H}}\mathbf{V}_r\right) \boldsymbol{\Sigma}_r^{-1} \cancel{\left(\mathbf{U}_r^{\mathsf{H}}\mathbf{e} - \mathbf{U}_r^{\mathsf{H}}\mathbf{e}\right)} = \mathbf{0}
\end{aligned} \tag{A.10c}$$

$$\begin{aligned}
\mathbf{f}^{\mathsf{H}}\mathbf{G} &= \mathbf{f}^{\mathsf{H}} \left(\mathbf{V}_r - \mathbf{V}_k \left(\mathbf{f}^{\mathsf{H}}\mathbf{V}_k\right)^{-1} \mathbf{f}^{\mathsf{H}}\mathbf{V}_r\right) \boldsymbol{\Sigma}_r^{-1} \left(\mathbf{U}_r^{\mathsf{H}} - \mathbf{U}_r^{\mathsf{H}}\mathbf{e} \left(\mathbf{U}_k^{\mathsf{H}}\mathbf{e}\right)^{-1} \mathbf{U}_k^{\mathsf{H}}\right) \\
&= \left(\mathbf{f}^{\mathsf{H}}\mathbf{V}_r - \mathbf{f}^{\mathsf{H}}\mathbf{V}_k \left(\mathbf{f}^{\mathsf{H}}\mathbf{V}_k\right)^{-1} \mathbf{f}^{\mathsf{H}}\mathbf{V}_r\right) \boldsymbol{\Sigma}_r^{-1} \left(\mathbf{U}_r^{\mathsf{H}} - \mathbf{U}_r^{\mathsf{H}}\mathbf{e} \left(\mathbf{U}_k^{\mathsf{H}}\mathbf{e}\right)^{-1} \mathbf{U}_k^{\mathsf{H}}\right) \\
&= \cancel{\left(\mathbf{f}^{\mathsf{H}}\mathbf{V}_r - \mathbf{f}^{\mathsf{H}}\mathbf{V}_r\right)} \boldsymbol{\Sigma}_r^{-1} \left(\mathbf{U}_r^{\mathsf{H}} - \mathbf{U}_r^{\mathsf{H}}\mathbf{e} \left(\mathbf{U}_k^{\mathsf{H}}\mathbf{e}\right)^{-1} \mathbf{U}_k^{\mathsf{H}}\right) = \mathbf{0}
\end{aligned} \tag{A.10d}$$

$$\mathbf{f}^{\mathsf{H}}\mathbf{x} = \mathbf{f}^{\mathsf{H}}\mathbf{V}_k \left(\mathbf{f}^{\mathsf{H}}\mathbf{V}_k\right)^{-1} = \mathbf{I} \tag{A.10e}$$

$$\mathbf{y}^{\mathsf{H}}\mathbf{e} = \left(\mathbf{U}_k^{\mathsf{H}}\mathbf{e}\right)^{-1} \mathbf{U}_k^{\mathsf{H}}\mathbf{e} = \mathbf{I}. \tag{A.10f}$$

The property of Eq. (A.10d) is used in Eq. (13b).

A.2 Spectral decomposition

Alternatively, consider the spectral decomposition of the complex matrix $\mathbf{A}$ resulting from its eigenanalysis, namely

$$\mathbf{A} = \mathbf{X}\boldsymbol{\Lambda}\mathbf{X}^{-1} = \mathbf{X}\boldsymbol{\Lambda}\mathbf{Y}^{\mathsf{H}}, \tag{A.11}$$

where $\mathbf{X}$ and $\mathbf{Y} = \mathbf{X}^{-\mathsf{H}}$ respectively are the right and left eigenvector matrices and $\boldsymbol{\Lambda}$ is the diagonal matrix of the eigenvalues of $\mathbf{A}$, under the assumption that $\mathbf{A}$ is diagonalizable. Matrix $\mathbf{A}$ is assumed to be singular; thus, $k = n - r$ eigenvalues are zero. Assuming the r non-zero eigenvalues are listed first, the spectral decomposition can be rewritten as

$$\mathbf{A} = \begin{bmatrix} \mathbf{X}_r & \mathbf{X}_k \end{bmatrix} \begin{bmatrix} \boldsymbol{\Lambda}_r & \mathbf{0} \\ \mathbf{0} & \mathbf{0} \end{bmatrix} \begin{bmatrix} \mathbf{Y}_r^{\mathsf{H}} \\ \mathbf{Y}_k^{\mathsf{H}} \end{bmatrix} = \mathbf{X}_r \boldsymbol{\Lambda}_r \mathbf{Y}_r^{\mathsf{H}} \tag{A.12}$$

with $\mathbf{X}_r, \mathbf{Y}_r \in \mathbb{C}^{n\times r}$ and $\mathbf{X}_k, \mathbf{Y}_k \in \mathbb{C}^{k\times k}$, and $\mathbf{Y}^{\mathsf{H}}\mathbf{X} = \mathbf{I}$, which implies $\mathbf{Y}_r^{\mathsf{H}}\mathbf{X}_r = \mathbf{I}$, $\mathbf{Y}_k^{\mathsf{H}}\mathbf{X}_k = \mathbf{I}$, $\mathbf{Y}_r^{\mathsf{H}}\mathbf{X}_k = \mathbf{0}$, and $\mathbf{Y}_k^{\mathsf{H}}\mathbf{X}_r = \mathbf{0}$, and finally $\boldsymbol{\Lambda}_r \in \mathbb{C}^{r\times r}$ diagonal, with non-zero diagonal elements.

We can rewrite matrix $\tilde{\mathbf{A}}$ as

$$\tilde{\mathbf{A}} = \mathbf{A} + \mathbf{e}\mathbf{D}\mathbf{f}^{\mathsf{H}} = \mathbf{X}_r \boldsymbol{\Lambda}_r \mathbf{Y}_r^{\mathsf{H}} + \mathbf{e}\mathbf{D}\mathbf{f}^{\mathsf{H}} = \begin{bmatrix} \mathbf{X}_r & \mathbf{e} \end{bmatrix} \begin{bmatrix} \boldsymbol{\Lambda}_r & \mathbf{0} \\ \mathbf{0} & \mathbf{D} \end{bmatrix} \begin{bmatrix} \mathbf{Y}_r^{\mathsf{H}} \\ \mathbf{f}^{\mathsf{H}} \end{bmatrix}. \tag{A.13}$$

Under the assumption that the columns of $\mathbf{A}$ and $\mathbf{e}$ span $\mathbb{C}^n$, matrix $[\mathbf{X}_r, \mathbf{e}]$ is invertible; in fact,

$$\begin{bmatrix} \mathbf{Y}_r^{\mathsf{H}} \\ \mathbf{Y}_k^{\mathsf{H}} \end{bmatrix} \begin{bmatrix} \mathbf{X}_r & \mathbf{e} \end{bmatrix} = \begin{bmatrix} \mathbf{Y}_r^{\mathsf{H}}\mathbf{X}_r & \mathbf{Y}_r^{\mathsf{H}}\mathbf{e} \\ \cancel{\mathbf{Y}_k^{\mathsf{H}}\mathbf{X}_r} & \mathbf{Y}_k^{\mathsf{H}}\mathbf{e} \end{bmatrix} = \begin{bmatrix} \mathbf{I} & \mathbf{Y}_r^{\mathsf{H}}\mathbf{e} \\ \mathbf{0} & \mathbf{Y}_k^{\mathsf{H}}\mathbf{e} \end{bmatrix}, \tag{A.14}$$

i.e.,

$$\begin{bmatrix} \mathbf{X}_r & \mathbf{e} \end{bmatrix}^{-1} = \begin{bmatrix} \mathbf{I} & \mathbf{Y}_r^{\mathsf{H}}\mathbf{e} \\ \mathbf{0} & \mathbf{Y}_k^{\mathsf{H}}\mathbf{e} \end{bmatrix}^{-1} \begin{bmatrix} \mathbf{Y}_r^{\mathsf{H}} \\ \mathbf{Y}_k^{\mathsf{H}} \end{bmatrix} = \begin{bmatrix} \mathbf{Y}_r^{\mathsf{H}} - \mathbf{Y}_r^{\mathsf{H}}\mathbf{e}\left(\mathbf{Y}_k^{\mathsf{H}}\mathbf{e}\right)^{-1}\mathbf{Y}_k^{\mathsf{H}} \\ \left(\mathbf{Y}_k^{\mathsf{H}}\mathbf{e}\right)^{-1}\mathbf{Y}_k^{\mathsf{H}} \end{bmatrix}. \tag{A.15}$$

Similarly, under the assumption that the columns of $\mathbf{A}^{\mathsf{H}}$ and $\mathbf{f}$ span $\mathbb{C}^n$, matrix $[\mathbf{Y}_r, \mathbf{f}]^{\mathsf{H}}$ is invertible; in fact,

$$\begin{bmatrix} \mathbf{Y}_r & \mathbf{f} \end{bmatrix}^{-\mathsf{H}} = \begin{bmatrix} \mathbf{Y}_r^{\mathsf{H}} \\ \mathbf{f}^{\mathsf{H}} \end{bmatrix}^{-1} = \begin{bmatrix} \mathbf{X}_r - \mathbf{X}_k\left(\mathbf{f}^{\mathsf{H}}\mathbf{X}_k\right)^{-1}\mathbf{f}^{\mathsf{H}}\mathbf{X}_r & \mathbf{X}_k\left(\mathbf{f}^{\mathsf{H}}\mathbf{X}_k\right)^{-1} \end{bmatrix}. \tag{A.16}$$

The inverse of matrix $\tilde{\mathbf{A}}$ is thus

$$\begin{aligned} \tilde{\mathbf{A}}^{-1} &= \begin{bmatrix} \mathbf{Y}_r^{\mathsf{H}} \\ \mathbf{f}^{\mathsf{H}} \end{bmatrix}^{-1} \begin{bmatrix} \boldsymbol{\Lambda}_r & \mathbf{0} \\ \mathbf{0} & \mathbf{D} \end{bmatrix}^{-1} \begin{bmatrix} \mathbf{X}_r & \mathbf{e} \end{bmatrix}^{-1} \\ &= \begin{bmatrix} \mathbf{X}_r - \mathbf{X}_k\left(\mathbf{f}^{\mathsf{H}}\mathbf{X}_k\right)^{-1}\mathbf{f}^{\mathsf{H}}\mathbf{X}_r & \mathbf{X}_k\left(\mathbf{f}^{\mathsf{H}}\mathbf{X}_k\right)^{-1} \end{bmatrix} \begin{bmatrix} \boldsymbol{\Lambda}_r^{-1} & \mathbf{0} \\ \mathbf{0} & \mathbf{D}^{-1} \end{bmatrix} \\ &\quad \times \begin{bmatrix} \mathbf{Y}_r^{\mathsf{H}} - \mathbf{Y}_r^{\mathsf{H}}\mathbf{e}\left(\mathbf{Y}_k^{\mathsf{H}}\mathbf{e}\right)^{-1}\mathbf{Y}_k^{\mathsf{H}} \\ \left(\mathbf{Y}_k^{\mathsf{H}}\mathbf{e}\right)^{-1}\mathbf{Y}_k^{\mathsf{H}} \end{bmatrix} \\ &= \left(\mathbf{X}_r - \mathbf{X}_k\left(\mathbf{f}^{\mathsf{H}}\mathbf{X}_k\right)^{-1}\mathbf{f}^{\mathsf{H}}\mathbf{X}_r\right)\boldsymbol{\Lambda}_r^{-1}\left(\mathbf{Y}_r^{\mathsf{H}} - \mathbf{Y}_r^{\mathsf{H}}\mathbf{e}\left(\mathbf{Y}_k^{\mathsf{H}}\mathbf{e}\right)^{-1}\mathbf{Y}_k^{\mathsf{H}}\right) \\ &\quad + \mathbf{X}_k\left(\mathbf{f}^{\mathsf{H}}\mathbf{X}_k\right)^{-1}\mathbf{D}^{-1}\left(\mathbf{Y}_k^{\mathsf{H}}\mathbf{e}\right)^{-1}\mathbf{Y}_k^{\mathsf{H}} \\ &= \mathbf{G} + \mathbf{x}\mathbf{D}^{-1}\mathbf{y}^{\mathsf{H}}, \end{aligned} \tag{A.17}$$

with

$$\mathbf{G} = \left(\mathbf{X}_r - \mathbf{X}_k\left(\mathbf{f}^{\mathsf{H}}\mathbf{X}_k\right)^{-1}\mathbf{f}^{\mathsf{H}}\mathbf{X}_r\right)\boldsymbol{\Lambda}_r^{-1}\left(\mathbf{Y}_r^{\mathsf{H}} - \mathbf{Y}_r^{\mathsf{H}}\mathbf{e}\left(\mathbf{Y}_k^{\mathsf{H}}\mathbf{e}\right)^{-1}\mathbf{Y}_k^{\mathsf{H}}\right) \tag{A.18a}$$

$$\mathbf{x} = \mathbf{X}_k\left(\mathbf{f}^{\mathsf{H}}\mathbf{X}_k\right)^{-1} \tag{A.18b}$$

$$\mathbf{y} = \mathbf{Y}_k\left(\mathbf{e}^{\mathsf{H}}\mathbf{Y}_k\right)^{-1}. \tag{A.18c}$$

The elements of the inverse of matrix $\tilde{\mathbf{A}}$ from this formulation are identical to those of Eq. (A.9a)–(A.9c). Nonetheless, it is again worth noticing that, along the lines of Corollary 1

in [38],

$$\mathbf{A}\mathbf{x} = \mathbf{X}_r \boldsymbol{\Lambda}_r \cancel{\mathbf{Y}_r^{\mathrm{H}} \mathbf{X}_k} \left(\mathbf{f}^{\mathrm{H}} \mathbf{X}_k\right)^{-1} = \mathbf{0} \tag{A.19a}$$

$$\mathbf{y}^{\mathrm{H}} \mathbf{A} = \left(\mathbf{Y}_k^{\mathrm{H}} \mathbf{e}\right)^{-1} \cancel{\mathbf{Y}_k^{\mathrm{H}} \mathbf{X}_r} \boldsymbol{\Lambda}_r \mathbf{Y}_r^{\mathrm{H}} = \mathbf{0} \tag{A.19b}$$

$$\begin{aligned} \mathbf{G}\mathbf{e} &= \left(\mathbf{X}_r - \mathbf{X}_k \left(\mathbf{f}^{\mathrm{H}} \mathbf{X}_k\right)^{-1} \mathbf{f}^{\mathrm{H}} \mathbf{X}_r\right) \boldsymbol{\Lambda}_r^{-1} \left(\mathbf{Y}_r^{\mathrm{H}} - \mathbf{Y}_r^{\mathrm{H}} \mathbf{e} \left(\mathbf{Y}_k^{\mathrm{H}} \mathbf{e}\right)^{-1} \mathbf{Y}_k^{\mathrm{H}}\right) \mathbf{e} \\ &= \left(\mathbf{X}_r - \mathbf{X}_k \left(\mathbf{f}^{\mathrm{H}} \mathbf{X}_k\right)^{-1} \mathbf{f}^{\mathrm{H}} \mathbf{X}_r\right) \boldsymbol{\Lambda}_r^{-1} \left(\mathbf{Y}_r^{\mathrm{H}} \mathbf{e} - \mathbf{Y}_r^{\mathrm{H}} \mathbf{e} \left(\mathbf{Y}_k^{\mathrm{H}} \mathbf{e}\right)^{-1} \mathbf{Y}_k^{\mathrm{H}} \mathbf{e}\right) \\ &= \left(\mathbf{X}_r - \mathbf{X}_k \left(\mathbf{f}^{\mathrm{H}} \mathbf{X}_k\right)^{-1} \mathbf{f}^{\mathrm{H}} \mathbf{X}_r\right) \boldsymbol{\Lambda}_r^{-1} \cancel{\left(\mathbf{Y}_r^{\mathrm{H}} \mathbf{e} - \mathbf{Y}_r^{\mathrm{H}} \mathbf{e}\right)} = \mathbf{0} \end{aligned} \tag{A.19c}$$

$$\begin{aligned} \mathbf{f}^{\mathrm{H}} \mathbf{G} &= \mathbf{f}^{\mathrm{H}} \left(\mathbf{X}_r - \mathbf{X}_k \left(\mathbf{f}^{\mathrm{H}} \mathbf{X}_k\right)^{-1} \mathbf{f}^{\mathrm{H}} \mathbf{X}_r\right) \boldsymbol{\Lambda}_r^{-1} \left(\mathbf{Y}_r^{\mathrm{H}} - \mathbf{Y}_r^{\mathrm{H}} \mathbf{e} \left(\mathbf{Y}_k^{\mathrm{H}} \mathbf{e}\right)^{-1} \mathbf{Y}_k^{\mathrm{H}}\right) \\ &= \left(\mathbf{f}^{\mathrm{H}} \mathbf{X}_r - \mathbf{f}^{\mathrm{H}} \mathbf{X}_k \left(\mathbf{f}^{\mathrm{H}} \mathbf{X}_k\right)^{-1} \mathbf{f}^{\mathrm{H}} \mathbf{X}_r\right) \boldsymbol{\Lambda}_r^{-1} \left(\mathbf{Y}_r^{\mathrm{H}} - \mathbf{Y}_r^{\mathrm{H}} \mathbf{e} \left(\mathbf{Y}_k^{\mathrm{H}} \mathbf{e}\right)^{-1} \mathbf{Y}_k^{\mathrm{H}}\right) \\ &= \cancel{\left(\mathbf{f}^{\mathrm{H}} \mathbf{X}_r - \mathbf{f}^{\mathrm{H}} \mathbf{X}_r\right)} \boldsymbol{\Sigma}_r^{-1} \left(\mathbf{Y}_r^{\mathrm{H}} - \mathbf{Y}_r^{\mathrm{H}} \mathbf{e} \left(\mathbf{Y}_k^{\mathrm{H}} \mathbf{e}\right)^{-1} \mathbf{Y}_k^{\mathrm{H}}\right) = \mathbf{0} \end{aligned} \tag{A.19d}$$

$$\mathbf{f}^{\mathrm{H}} \mathbf{x} = \mathbf{f}^{\mathrm{H}} \mathbf{X}_k \left(\mathbf{f}^{\mathrm{H}} \mathbf{X}_k\right)^{-1} = \mathbf{I} \tag{A.19e}$$

$$\mathbf{y}^{\mathrm{H}} \mathbf{e} = \left(\mathbf{Y}_k^{\mathrm{H}} \mathbf{e}\right)^{-1} \mathbf{Y}_k^{\mathrm{H}} \mathbf{e} = \mathbf{I}. \tag{A.19f}$$

The property of Eq. (A.19d) is used in Eq. (13b).

Author contributions All authors worked on the conceptualization. B.L. and P.M. wrote the manuscript text. B.L. performed the calculations. All authors analyzed the results and reviewed the manuscript.

Funding information Open access funding provided by Politecnico di Milano within the CRUI-CARE Agreement. The first author is supported by the China Scholarship Council program (No. 202306830074). The authors also acknowledge the support of the National Natural Science Foundation of China (No. 12272169).

Data availability No datasets were generated or analysed during the current study.

Declarations

Competing interests The third author, Pierangelo Masarati, is an Associate Editor of the journal Multibody System Dynamics but has not been involved in the review of this manuscript. The authors have no other potential conflicts of interest to declare that are relevant to the content of this article.

References

1. Mottershead, J.E., Link, M., Friswell, M.I.: The sensitivity method in finite element model updating: a tutorial. Mech. Syst. Signal Process. **25**(7), 2275–2296 (2011). https://doi.org/10.1016/j.ymssp.2010.10.012

2. Nelson, R.B.: Simplified calculation of eigenvector derivatives. AIAA J. **14**(9), 1201–1205 (1976). https://doi.org/10.2514/3.7211
3. Fox, R.L., Kapoor, M.P.: Rates of change of eigenvalues and eigenvectors. AIAA J. **6**(12), 2426–2429 (1968). https://doi.org/10.2514/3.5008
4. van Keulen, F., Haftka, R.T., Kim, N.H.: Review of options for structural design sensitivity analysis. Part 1: linear systems. Comput. Methods Appl. Mech. Eng. **194**(30), 3213–3243 (2005). https://doi.org/10.1016/j.cma.2005.02.002
5. Hannemann, R., Marquardt, W., Naumann, U., Gendler, B.: Discrete first- and second-order adjoints and automatic differentiation for the sensitivity analysis of dynamic models. Proc. Comput. Sci. **1**(1), 297–305 (2010). https://doi.org/10.1016/j.procs.2010.04.033
6. Callejo, A., García de Jalón, J.: A hybrid direct-automatic differentiation method for the computation of independent sensitivities in multibody systems. Int. J. Numer. Methods Eng. **100**(12), 933–952 (2014). https://doi.org/10.1002/nme.4804
7. Fan, X., Rong, B., Lin, X., Sun, A.: Multibody dynamics sensitivity analysis by discrete time transfer matrix method. In: 1st International Conference on Mechanical System Dynamics (ICMSD 2022), vol. 2022, pp. 1447–1452 (2022). https://doi.org/10.1049/icp.2022.2024
8. Schulz, C., Graneß, H., Weinzierl, S., Nicklas, J.: Eigenvalue perturbation in drivetrain analysis and optimization (2025). https://doi.org/10.21203/rs.3.rs-6368754/v1
9. Ruiz, D., Bellido, J.C., Donoso, A.: Eigenvector sensitivity when tracking modes with repeated eigenvalues. Comput. Methods Appl. Mech. Eng. **326**, 338–357 (2017). https://doi.org/10.1016/j.cma.2017.07.031
10. Yang, Q., Peng, X., Yang, Q., Peng, X.: An exact method for calculating the eigenvector sensitivities. Appl. Sci. **10**(7) (2020). https://doi.org/10.3390/app10072577
11. He, S., Jonsson, E., Martins, J.R.R.A.: Derivatives for eigenvalues and eigenvectors via analytic reverse algorithmic differentiation. AIAA J. **60**(4), 2654–2667 (2022). https://doi.org/10.2514/1.J060726
12. Held, A.: On design sensitivities in the structural analysis and optimization of flexible multibody systems. Multibody Syst. Dyn. **54**(1), 53–74 (2022). https://doi.org/10.1007/s11044-021-09800-1
13. López Varela, Á., Dopico Dopico, D., Luaces Fernández, A.: An analytical approach to the sensitivity analysis of semi-recursive ODE formulations for multibody dynamics. Comput. Struct. **308**, 107642 (2025). https://www.sciencedirect.com/science/article/pii/S0045794924003717
14. Tu, T., Wang, G., Rui, X., Zhou, Q., Miao, Y.: Direct differentiation method for sensitivity analysis based on transfer matrix method for multibody systems. Int. J. Numer. Methods Eng. **115**(13), 1601–1622 (2018). https://doi.org/10.1002/nme.5910
15. Haug, E.J., Choi, K.K.: Structural design sensitivity analysis with generalized global stiffness and mass matrices. AIAA J. **22**(9), 1299–1303 (1984). https://doi.org/10.2514/3.8776
16. Bestle, D., Seybold, J.: Sensitivity analysis of constrained multibody systems. Arch. Appl. Mech. **62**(3), 181–190 (1992). https://doi.org/10.1007/BF00787958
17. Zhang, Z., Mao, Y., Su, X., Yuan, X.: Adjoint-based boundary condition sensitivity analysis. AIAA J. **60**(6), 3517–3527 (2022). https://doi.org/10.2514/1.J061307
18. Holzer, H.: Die Berechnung der Drehsenwingungen. Springer, Berlin (1921). https://doi.org/10.1007/978-3-642-51387-9
19. Myklestad, N.O.: New method of calculating natural modals of coupled bending-torsion vibration of beams. Trans. Am. Soc. Mech. Eng. **67**(1), 61–67 (1945). https://doi.org/10.1115/1.4018171
20. Rui, X., He, B., Lu, Y., Lu, W., Wang, G.: Discrete time transfer matrix method for multibody system dynamics. Multibody Syst. Dyn. **14**(3–4), 317–344 (2005). https://doi.org/10.1007/s11044-005-5006-1
21. Rui, X., Wang, G., Zhang, J.: Transfer Matrix Method for Multibody Systems — Theory and Applications. Wiley, Singapore (2019). https://doi.org/10.1002/9781118724811
22. Rui, X., Abbas, L.K., Yang, F., Wang, G., Yu, H., Wang, Y.: Flapwise vibration computations of coupled helicopter rotor/fuselage: application of multibody system dynamics. AIAA J. **56**(2), 818–835 (2018). https://doi.org/10.2514/1.J056591
23. Yu, H., Rui, X.: Study on launch dynamics of self-propelled artillery based on transfer matrix method of multibody system. Adv. Mech. Eng. **6**, 308049 (2014). https://doi.org/10.1155/2014/308049
24. Murthy, V.R., Lin, Y.-A., O'Hara, S.W.: Sensitivity derivatives of eigendata of one-dimensional structural systems. AIAA J. **38**(1), 115–122 (2000). https://doi.org/10.2514/2.931
25. Wang, X., Rui, X., Yang, F., Zhou, Q.: Launch dynamics modeling and simulation of vehicular missile system. J. Guid. Control Dyn. **41**(6), 1370–1379 (2018). https://doi.org/10.2514/1.G003363
26. Wang, X., Song, L., Xia, P.: A novel modeling strategy for the dynamical analysis of coupled coaxial rotors/auxiliary propeller/drive train system. J. Am. Helicopter Soc. **68**(1), 012003 (2023). https://doi.org/10.4050/JAHS.68.012003
27. Rui, X., Zhang, J., Wang, X., Rong, B., He, B., Jin, Z.: Multibody system transfer matrix method: the past, the present, and the future. Int. J. Mech. Syst. Dyn. **2**(1), 3–26 (2022). https://doi.org/10.1002/msd2.12037

28. Wang, X., Xia, P.: Novel modeling and vibration analysis method on a helicopter drive train system. AIAA J. **60**(7), 4288–4301 (2022). https://doi.org/10.2514/1.J061493
29. Wang, J., Rui, X., Wang, X., Zhang, J., Zhou, Q., Gu, J.: Eigenvalue analysis of planar linear multibody system under conservative force based on the transfer matrix method. Int. J. Mech. Syst. Dyn. **3**(1), 12–24 (2023). https://doi.org/10.1002/msd2.12048
30. Ling, M., Yuan, L., Zeng, T., Zhang, X.: Enabling the transfer matrix method to model serial–parallel compliant mechanisms including curved flexure beams. Int. J. Mech. Syst. Dyn. **4**(1), 48–62 (2024). https://doi.org/10.1002/msd2.12097
31. Dai, W., Carboni, B., Quaranta, G., Pan, Y., Lacarbonara, W.: Nonlinear response of a multidirectional negative-stiffness isolation system via semirecursive multibody dynamic approach. Int. J. Mech. Syst. Dyn. **4**(3), 258–277 (2024). https://doi.org/10.1002/msd2.12118
32. Bestle, D.: Eigenvalue sensitivity analysis based on the transfer matrix method. Int. J. Mech. Syst. Dyn. **1**(1), 96–107 (2021). https://doi.org/10.1002/msd2.12016
33. Wang, X., Rui, X., Gu, J., Yang, F.: Sensitivity analysis method for frequency response function based on extended transfer matrix method for linear multibody systems. In: Proceedings of 1st International Conference on Mechanical System Dynamics, vol. 2022, pp. 351–358. IET (2022). https://doi.org/10.1049/icp.2022.1751
34. Wang, J., Rui, X., He, B., Wang, X., Xie, K.: A fast calculation method for sensitivity analysis based on multibody system transfer matrix method. Int. J. Appl. Mech. **17**(3), 2550008 (2025). https://doi.org/10.1142/S1758825125500085
35. Rui, X., Zhang, J., Zhou, Q.: Automatic deduction theorem of overall transfer equation of multibody system. Adv. Mech. Eng. **6**, 378047 (2014). https://doi.org/10.1155/2014/378047
36. Masarati, P.: Eigensolution sensitivity revisited. Under review
37. Brandt Petersen, K., Pedersen, M.S.: The Matrix Cookbook. (2008)
38. Eriksson, S., Nordqvist, J.: Inverting the sum of two singular matrices. Results Appl. Math. **22**, 100463 (2024). https://doi.org/10.1016/j.rinam.2024.100463
39. Wu, J.S., Chen, C.H.: Torsional vibration analysis of gear-branched systems by finite element method. J. Sound Vib. **240**(1), 159–182 (2001). https://doi.org/10.1006/jsvi.2000.3197
40. Zhong-Sheng, L., Su-Huan, C., Tao, X.: Derivatives of eigenvalues for torsional vibration of geared shaft systems. J. Vib. Acoust. **115**(3), 277–279 (1993). https://doi.org/10.1115/1.2930345